

SMOS L1 Prototype
ADF Set Description / Table Generation
Requirements Document

Code : SO-TGRD-DME-L1PP-0023
Issue : 3.0
Date : 30/11/12

| | Name | Function | Signature |
|--------------------|-------------|--------------------|------------------|
| Prepared by | A.Gutiérrez | Project Engineer | |
| | R.Castro | Project Engineer | |
| Checked by | A.Gutiérrez | Quality A. Manager | |
| Approved by | J. Barbosa | Project Manager | |

DEIMOS Engenharia
Av. D. João II, Lote 1.17, Torre Zen, 10º
1998-023 Lisboa, PORTUGAL
Tel: +351 21 893 3013
Fax: +351 21 896 9099
E-mail: <mailto:deimos@deimos.com.pt>

© DEIMOS Engenharia 2012

This page intentionally left blank

Document Information

| Contract Data | Classification |
|-------------------------------------|--|
| Contract Number: 4000101241/10/I-AM | Internal <input checked="" type="checkbox"/> |
| Contract Issuer: ESA | Public <input type="checkbox"/> |
| | Industry <input type="checkbox"/> |
| | Confidential <input type="checkbox"/> |

| Internal Distribution | | |
|-----------------------|------|--------|
| Name | Unit | Copies |
| | | |

| External Distribution | | |
|-----------------------|--------------|--------|
| Name | Organisation | Copies |
| Jean-Claude Debruyne | ESA | 1 |
| Steven Delwart | ESA | 1 |

| Archiving | |
|-----------------|--|
| Word Processor: | MS Word 2000 |
| File Name: | SO-TGRD-DME-L1PP-0023-ADF-set-description_TGRD.doc |
| Archive Code: | SO-TGRD-DME-L1PP-0023 |

Document Status Log

| Issue | Change description | Date | Approved |
|-------|---|------------|----------|
| Draft | First version of the document | 12-05-2006 | |
| 1.0 | Version delivered for the OSAT | 05-06-2006 | |
| 1.1 | Version delivered after the OSAT | 29-06-2006 | |
| 1.2 | Updated Land/Sea Mask Auxiliary Data File. Corrected Total Size of Land/Mask and Galaxy Map ADFs for consistency. | 20-07-2006 | |
| 1.3 | Added ADF headers to ADF Package | 26-07-2006 | |
| 1.4 | Update for L1OP CDR | 26-10-2006 | |
| 2.0 | Update for L1PP V2R | 17-11-2006 | |
| 2.1 | Update for L1PP V3R | 09-04-2007 | |
| 2.2 | Update for L1PP V3.5R | 17-07-2007 | |
| 2.3 | Update for L1PP V4R | 26-11-2007 | |
| 2.4 | Update for L1PP V5R | 04-04-2008 | |
| 2.5 | Update for L1PP V6R | 25-07-2008 | |
| 2.6 | Update for L1PP V6.5R | 22-10-2008 | |
| 2.7 | Update for L1PP v3.1.0 | 19-05-2009 | |
| 2.8 | Update for L1PP v2.2.0 | 24-07-2009 | |
| 2.9 | Update for L1PP v3.2.0 | 24-09-2009 | |
| 2.10 | Update for L1PP v3.3.0 | 26-03-2010 | |
| 2.11 | Update for L1PP v3.4.0 | 31-05-2010 | |
| 2.12 | Updated after review for the Maintenance Phase and for L1PP v3.5.0 | 29-10-2010 | |
| 2.13 | Update for L1PP v5.0.0 | 20-05-2011 | |
| 2.14 | Update for L1PP v5.5.0 | 29-11-2011 | |
| 3.0 | Update for L1PP v6.0.0 | 30-11-2012 | |
| | Moved contents related to AUX file generation from L1b DPM | | |
| | Re-versioning for L1OP contract and renamed document to reflect the new scope | | |
| | <u>Changed document ID from SO-TDD-DME-L1PP-0023-ADF-set-description to SO-TGRD-DME-L1PP-0023-ADF-set-description</u> | | |

Table of Contents

| | |
|--|-----------|
| 1. INTRODUCTION | 9 |
| 1.1. Purpose and Scope | 9 |
| 1.2. Acronyms and Abbreviations | 9 |
| 1.3. Applicable and Reference Documents | 9 |
| 1.3.1. Applicable Documents | 9 |
| 1.3.2. Reference Documents | 10 |
| 2. Overview | 12 |
| 3. ADF Generation Procedures | 13 |
| 3.1. AUX_GMAT | 13 |
| 3.1.1. System Response definition | 13 |
| 3.1.2. On-ground characterised G-matrix | 21 |
| 3.1.2.1. Antenna Patterns | 22 |
| 3.1.2.2. Fringe Wash Function | 23 |
| 3.1.2.3. LICEF Spatial Coordinates | 24 |
| 3.1.3. Expanded Hexagonal Domain in the G-matrix | 24 |
| 3.1.4. System Response Function Mathematical Inversion | 25 |
| 3.1.5. Implementation | 25 |
| 3.1.5.1. Inputs | 27 |
| 3.1.5.2. Outputs | 27 |
| 3.1.5.3. List of Variables | 27 |
| 3.1.5.4. Implementation details | 28 |
| 3.2. AUX_JMAT | 34 |
| 3.2.1. J Matrix Inversion | 36 |
| 3.2.2. Implementation | 38 |
| 3.2.2.1. Inputs | 39 |
| 3.2.2.2. Outputs | 40 |
| 3.2.2.3. List of Variables | 40 |
| 3.2.2.4. Implementation details | 40 |
| 3.3. AUX_FTT | 45 |
| 3.4. AUX_RFI_LST | 46 |

| | |
|---|-----------|
| 3.5. RFI Detection Algorithms | 47 |
| 3.5.1. detectRFIPosition Function | 48 |
| 3.5.1.1. Inputs | 48 |
| 3.5.1.2. Outputs | 48 |
| 3.5.1.3. List of Variables | 48 |
| 3.5.1.4. Implementation | 49 |
| 3.5.2. logRFIPosition Function | 49 |
| 3.5.2.1. Inputs | 49 |
| 3.5.2.2. Outputs | 49 |
| 3.5.2.3. List of Variables | 50 |
| 3.5.2.4. Implementation | 50 |
| 4. L1PP ADF contents | 51 |
| 5. Auxiliary Data Files | 57 |
| 6. Annex: ADF Set Package contents | 66 |

List of Tables

| | |
|--|----|
| Table 1: Applicable Documents | 10 |
| Table 2: Reference Documents..... | 10 |
| Table 3: Elements with Antenna Patterns to be replaced | 23 |
| Table 4: On-ground characterised G-matrix Variable List..... | 28 |
| Table 5 – Baselines to be removed from J+ | 37 |
| Table 6: J Matrix Variable List..... | 40 |
| Table 7: detectRFIPosition variable list (Local variables list tbc)..... | 48 |
| Table 8: logRFIPosition variable list (Local variables list tbc)..... | 50 |
| Table 9: Generation Procedures Auxiliary Data Files..... | 51 |
| Table 10: List of Auxiliary Data Files..... | 57 |

1. INTRODUCTION

1.1. Purpose and Scope

This document describes the SMOS Level 1 Processor Prototype (L1PP) Auxiliary Data Files (ADFs). The purpose of the document is not to specify the format of the files but rather to identify the files that are delivered together with the prototype and provide a summary description of their contents¹.

As of L1PP v6.0.0, this document will also contain the description of the procedures needed to generate the ancillary files used during the L1 processing, such as the G/J+ matrices and Flat Target Transformation data.

This document is to be used by L1PP users as a support document and complements the Software User Manual Document [AD.9].

The files described in this document correspond to the baseline ADF Set 6.0.0.

1.2. Acronyms and Abbreviations

For the list of acronyms, please refer to the “Directory of Acronyms and abbreviations” [RD.1].

1.3. Applicable and Reference Documents

1.3.1. Applicable Documents

| Ref. | Code | Title | Issue |
|------|---------------------|--|-------------------------|
| AD.1 | Removed | | |
| AD.2 | ECSS-E-40B | ECSS E-40 Software Engineering Standards | |
| AD.3 | Removed | | |
| AD.4 | SO-DS-DME-L1PP-0007 | SMOS L1PP DPM L1a | 2.16 29/11/12 |
| AD.5 | SO-DS-DME-L1PP-0008 | SMOS L1PP DPM L1b | 2.16 29/11/12 |
| AD.6 | SO-DS-DME-L1PP-0009 | SMOS L1PP DPM L1c | 2.11 29/11/12 |

¹ For further information regarding the format of the files, please refer to AD13.

| Ref. | Code | Title | Issue |
|-------|---------------------|--|-------------------------|
| AD.7 | Removed | | |
| AD.8 | SO-TR-DME-L1PP-0018 | SMOS L1 Verification and Validation Plan | 2.12 29/11/12 |
| AD.9 | SO-UM-DME-L1PP-0016 | SMOS L1 Processor Prototype User Manual | 2.18 29/11/12 |
| AD.10 | Removed | | |
| AD.11 | SO-TN-UPC-PLM-0019 | SMOS In Orbit Calibration Plan Phase C-D | 1.5 17/01/07 |
| AD.12 | PE-TN-ESA-GS-001 | Earth Explorer Ground Segment File Format Standard | 1.4 |
| AD.13 | SO-TN-IDR-GS-0005 | SMOS Level 1 and Auxiliary Data Products Specifications | 5.24 06/12/12 |
| AD.14 | SO-SOW-ESA-GS-6647 | SMOS Expert Support Laboratories for the period 2010-2014 - ESL Level 1 Calibration and Reconstruction | 1.2 |

Table 1: Applicable Documents

1.3.2. Reference Documents

| Ref. | Code | Title | Issue |
|------|---------------------------|--|----------------------------|
| RD.1 | SO-LI-CASA-PLM-0094 | Directory of Acronyms and abbreviations | |
| RD.2 | SO-TN-DME-L1PP-0024 | SMOS L1 Full Polarisation Data Processing | 1.6 16/07/07 |
| RD.3 | Fernando Martin-Porqueras | Sky Visibilities Images Including Cross-polar and Polar Coordinates.pptx | 1.0 20/08/12 |
| RD.4 | SO-TN-UPC-PLM-0151 | Antenna pattern renormalization | 1.0 28/09/12 |
| RD.5 | SO-TN-UPC-PLM-0143 | ATBD for baseline based FTT | 1.0 29/03/12 |
| RD.6 | SO-DS-DME-L1PP-0202 | -SMOS L1PP Baselines Avoidance Algorithm | 1.1 24/07/09 |

Table 2: Reference Documents

2. OVERVIEW

The document is organized as follows:

- ❑ Section 3 presents the generation method and origin of data for each of the Auxiliary Data Files
- ❑ Section 4 presents a description of the Auxiliary Data Files used by the prototype.
- ❑ Section 5 lists the contents of the ADF Set 6.0.0.

3. ADF GENERATION PROCEDURES

In this section, we will describe the procedures needed to generate the ADF files used during processing. Either by a full algorithmic description, when the algorithm is implemented in the L1PP, or by a description on how the files were generated externally. The overall processing chain for L1 is presented in the following figure:

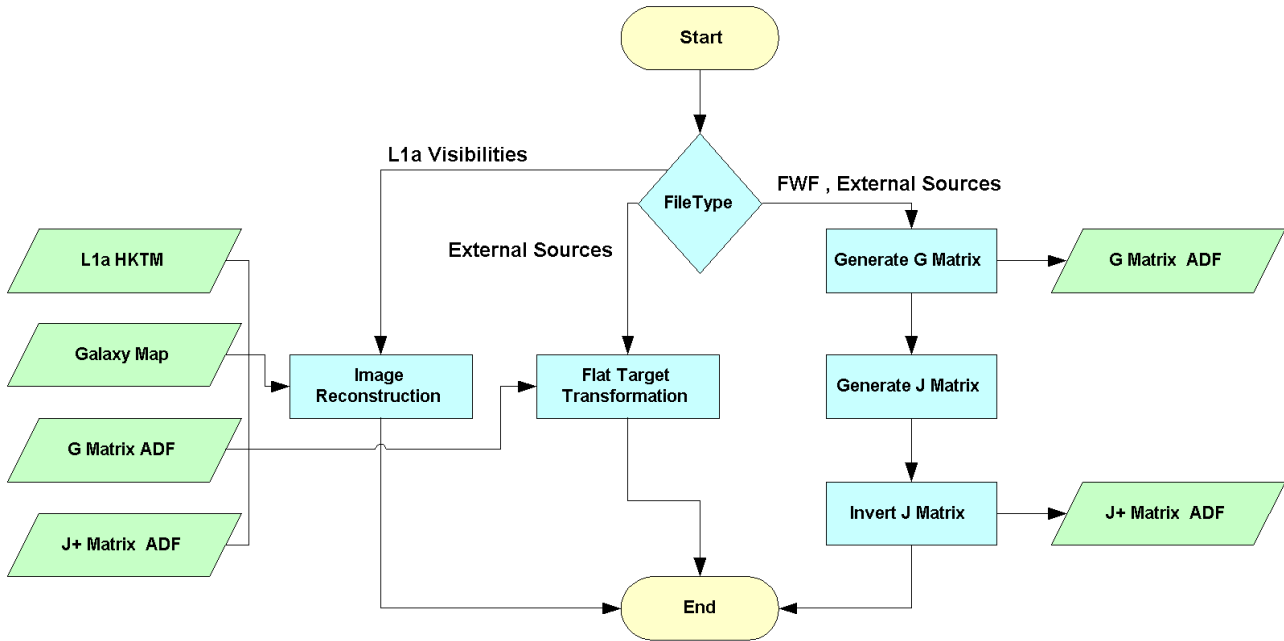


Figure 1: L1a to L1b Processing Flow

3.1. AUX_GMAT

3.1.1. System Response definition

The instrument's System Response Function is determined by the following equation:

$$V_j^q(u) = \iint_{\xi^2 + \eta^2 \leq 1} \frac{F_{n,j_1}^{p_1 q_1}(\xi) F_{n,j_2}^{p_2 q_2^*}(\xi) T_B^p(\xi) - T_{Rec} \delta_p \hat{r}_{kj}(-\Delta t) e^{-j2\pi f_0 \Delta t}}{\sqrt{\Omega_{j_1}^{p_1} \Omega_{j_2}^{p_2}} \zeta(\xi, \eta)} d\xi d\eta \quad \text{Eq. 1}$$

Where the following parameters are presented:

- $F_{n,j}^{pq}(\xi)$ is the normalised antenna radiation pattern of receiver j in polarisation p (co-polar if $q=p$ and cross-polar otherwise), expressed in cosine domain coordinates;

- Ω_j^p is the antenna solid angle of receiver j in polarisation p ;
- T_{Rec} is the averaged physical temperature of the receivers, multiplied by the Dirac delta δ_p to represent that it is not applicable when the polarisation indexes p_1 and p_2 are not equal (i.e. full-polarisation);
- $\zeta(\xi, \eta) \equiv \sqrt{1 - \xi^2 - \eta^2}$ is the *Obliquity Factor*;
- \hat{r}_{kj} is the Fringe Washing Function term, normalised at the origin, that accounts for decorrelation effects in the path of the correlated signals;
- $\Delta t \equiv u\xi + v\eta + w\zeta(\xi, \eta)$ is the *Delay Time*;
- $d\xi d\eta$ represents the area of each (ξ, η) spatial sample in the integration domain.

For the rest of the document, wherever these equations are used, the off-plane component entering the Fringe Wash function and the exponential has been simplified to keep each equation in a single line (OF is the Obliquity Factor).

This equation relates the visibilities measured by the instrument, with the Brightness Temperature scene that is being observed. Due to the nature of the double integral, and expressing the visibilities and Brightness Temperatures matrices as vectors, this relationship can be expressed as a matrix-vector multiplication, hereafter referring this matrix as G -matrix.

$$V(u) = G(u; \xi) T(\xi) \quad \text{Eq. 2}$$

This G -matrix is dependent on the antenna patterns, the fringe washing function, the (u, v) frequency samples of V (w is the out of plane coordinate) and the spatial samples (ξ, η) of BT. In order to obtain the Brightness Temperature distribution that generated a certain measured calibrated visibilities, it is only required to invert G by whatever method is more appropriate.

The first step is to specify the (u, v) frequency samples, and corresponding spatial samples (ξ, η) for the resolution selected, that match the instrument configuration. The (u, v) frequency samples are determined by the location of the receivers in the instrument, whereas the spatial samples are simply chosen based on the desired resolution. The preferred option is to work with a resolution of 128x128 or 64x64 spatial samples. If greater resolution is desired, an interpolation may be performed after the reconstruction.

The visibilities measurements are taken at specific frequency samples. Being (x_1, y_1) and (x_2, y_2) the XY plane coordinates, and z_1, z_2 the off-plane coordinates of two antennas generating the visibility sample V_{12} , the corresponding frequency sample can be computed as:

$$(u_{12}, v_{12}, w_{12}) = \left(\frac{x_2 - x_1}{\lambda_0}, \frac{y_2 - y_1}{\lambda_0}, \frac{z_2 - z_1}{\lambda_0} \right) \quad \text{Eq. 3}$$

Where λ_0 is the wavelength value at the central frequency of operation ($\lambda_0 = \frac{c}{f_0}$), for a typical value of f_0 of 1413.5MHz.

Computation of the spatial coordinates is done in a hexagonal grid but put in a rectangular matrix, according to the following formulation for an array steering of 30°. The corresponding frequency coordinates are also shown. Steering 30° means that the instrument is oriented with one of its arms (arm B) oriented 30° with respect to the flight direction.

Their outputs are two matrices with the coordinates of all points in the spatial and frequency domains according to the resolution specified:

$$(u, v) = \left(\frac{d}{2}(k_1 + 2k_2), \frac{\sqrt{3}d}{2}k_1 \right)$$

$$(\xi, \eta) = \left(\frac{1}{N_T d}k_1, \frac{1}{\sqrt{3}N_T d}(k_1 + 2k_2) \right)$$

Eq. 4

Where N_T is the resolution required (typically 128), d is the distance between adjacent receivers in wavelengths (typically 0.875), and k_1 and k_2 are the indexes of the matrix from 0 to N_T-1 . It must be noticed that the computation has to be performed according to the “hexagonal quadrant” where the indexes are, since the centre baseline is the first element of the matrix; this accounts to subtracting N_T from the indexes depending on the part of the hexagon being retrieved.

Initially the G -matrix shall be defined as the mathematical operator required to transform the 2556 complex calibrated visibilities plus the zero frequency value measured through the NIR elements (2556+3), into the 128x128 reconstructed Brightness Temperature values.

The complete system can be described by a unique G -matrix, which takes as input the data produced in all polarisations (H, V and HV). This unique G -matrix includes the effect of cross-polarisation antenna patterns into the reconstruction. This G -matrix format is the same for all reconstruction methods; the only difference between reconstruction approaches lies in the external elements used to construct it.

If the level of cross-polarisation contamination can be disregarded, because its effect is negligible, this unique G -matrix could be split into three separate and smaller G -matrices, one for each polarisation.

The purpose of this matrix (or matrices) is to be used for computation of the J matrix operator, which is described in the next chapters.

The most complete G -matrix ($V=GT$) is built for the full polarisation processing case, as the dual polarisation G -matrix shall be a subset of it. The input data in the case of full polarisation are three vectors of calibrated visibilities: V_H with 2346 complex elements (2556 - NIR_XX_XX_V) plus 3 real elements from the NIR measurement, V_V with the same amount of values 2346 (2556 - NIR_XX_XX_H) complex + 3 real and V_{HV} with 3303 complex elements. For information on this last case of V_{HV} , please refer to the document [RD.2]. The total number of input real valued elements shall then be $(2346*2+3)*2+3303*2=15996$.

In order to understand the origin of these numbers, it must be clear that in H or V polarisation, the amount of signals correlated is always 72, but of these only 69 are in either H or V polarisation. The remaining 3 are signals being correlated by the LICEF-NIR receivers in the opposite polarisation, so

only $69 \times 68/2$ complex correlations are measured, which is the source for 2346. The NIR elements are also measuring the total power of the image, which is the source for the remaining 3 real elements.

The required output is the Brightness Temperature values in all polarisations. T_H and T_V are real valued, whereas T_{HV} is complex valued. Assuming a default size of 128×128 , the total number of output real valued elements is $128 \times 128 \times 4 = 65536$. Of course, the size can be reduced to 64×64 , although a bigger sampling grid means that more detail is introduced in the System Response Function by using a finer antenna pattern grid.

Thus, the unique G -matrix shall be composed by 15996 rows and 65536 columns with real valued elements. Using a real valued matrix is preferred as it reduces the size and ensures that the output in Brightness Temperatures for H and V is real valued.

Rows in the G -matrix are generated from particularising the general equation for a pair of LICEF receivers (k, j indexes) and polarisation values of the antenna patterns and Brightness Temperature (p, q indexes).

The rows shall be ordered as follows:

- The first $2346 \times 2 + 3$ rows shall correspond to H polarisation calibrated visibilities (p and q are H).
- The next $2346 \times 2 + 3$ rows shall correspond to V polarisation calibrated visibilities (p and q are V).
- The final 3303×2 rows shall correspond to HV polarisation calibrated visibilities (p is H and q is V).

In more detail and based on the following picture:

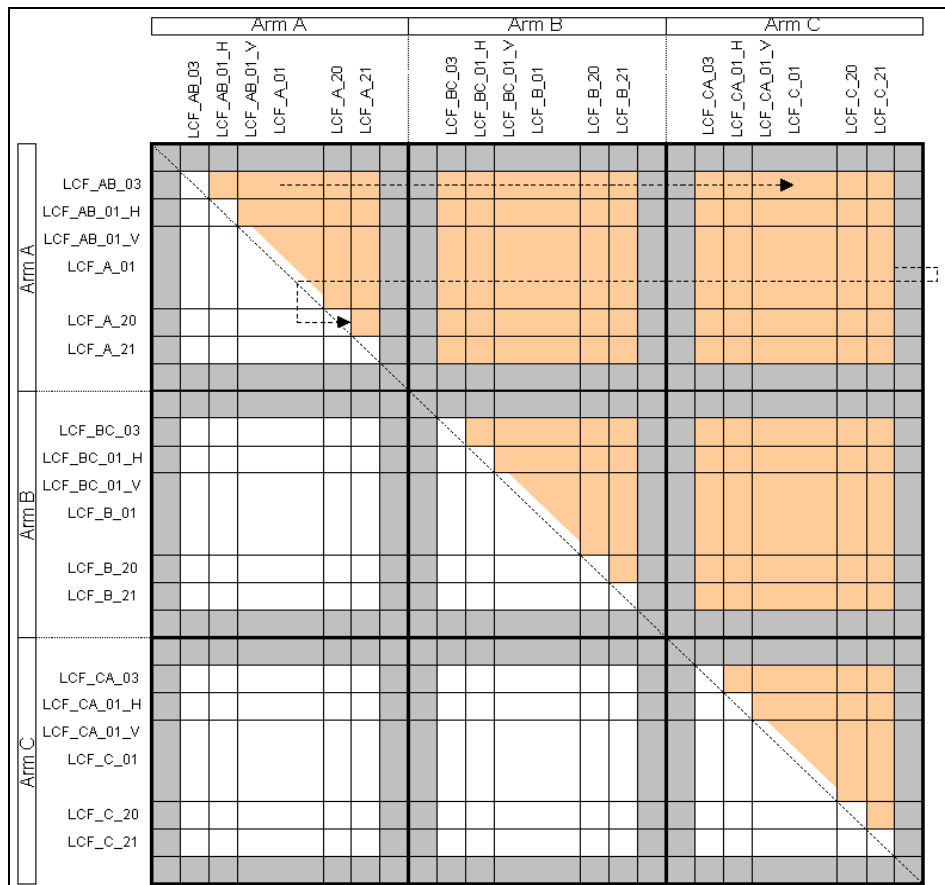


Figure 2: Calibrated Visibilities Matrix

- ❑ The first 3 rows shall correspond to the zero baselines as measured from the NIR for H polarisation. Order shall be first NIR_AB, then NIR_BC and last NIR_CA
- ❑ The next 2346 rows shall correspond to the real values of the H polarisation calibrated visibilities as received from the L1a products, and ordered in the same approach as shown in figure 11 in chapter 4.3.1.3 of [AD.13]. i.e. first element shall be calibrated visibility of LICEF_AB_03 against LICEF_AB_01_H, next shall be LICEF_AB_03 against LICEF_A_01, etc... until the sixty ninth element LICEF_AB_03 against LICEF_C_21. The next element shall then be LICEF_AB_01_H against LICEF_A_01, and so on until LICEF_AB_01 against LICEF_C_21. The next shall be LICEF_A_01 against LICEF_A_02, etc. until LICEF_A_02 against LICEF_C_21. This ordering shall continue until all LICEF correlations have been inserted, and not including correlations with LICEF_NIR in V polarisation (i.e. correlations with receivers LICEF_AB_01_V, LICEF_BC_01_V and LICEF_CA_01_V)
- ❑ The next 2346 rows shall correspond to the imaginary values of the H polarisation calibrated visibilities, following the same order as above.

- ❑ The next 3 rows shall correspond to the zero baselines as measured from the NIR for V polarisation. Order shall be first NIR_AB, then NIR_BC and last NIR_CA
- ❑ The next 2346 rows shall correspond to the real values of the V polarisation calibrated visibilities as received from the L1a products, and ordered in the same approach as shown in figure 11 of [AD.13]. i.e. first element shall be calibrated visibility of LICEF_AB_03 against LICEF_AB_01_V, next shall be LICEF_AB_03 against LICEF_A_01, etc... until the sixty ninth element LICEF_AB_03 against LICEF_C_21. The next element shall then be LICEF_AB_01_V against LICEF_A_01, and so on until LICEF_AB_01 against LICEF_C_21. The next shall be LICEF_A_01 against LICEF_A_02, etc. until LICEF_A_02 against LICEF_C_21. This ordering shall continue until all LICEF correlations have been inserted, and not including correlations with LICEF_NIR in H polarisation (i.e. correlations with receivers LICEF_AB_01_H, LICEF_BC_01_H and LICEF_CA_01_H).
- ❑ The next 2346 rows shall correspond to the imaginary values of the V polarisation calibrated visibilities, following the same order as above.
- ❑ The next 3303 rows shall correspond to the real values of the HV polarisation calibrated visibilities as received from the L1a products, and ordered according to the following approach. Please refer to figures 10 and 11 of [RD.2] (orange cells) for a visual representation of the description:
 - First 528 rows with calibrated visibilities of elements in Arm A in H polarisation against elements in Arm B in V polarisation. I.e. first LICEF_AB_03 against LICEF_BC_03, then LICEF_AB_03 against LICEF_BC_01_V, then LICEF_AB_03 against LICEF_B_01, until the 23rd element LICEF_AB_03 against LICEF_B_21. Next is LICEF_AB_01_H against LICEF_BC_03, then LICEF_AB_01_H against LICEF_B_01, and so on until all elements in arm B are correlated with LICEF_AB_01_H (Please note that this row does not include the correlation against LICEF_BC_01_V). This ordering continues until the last element correlated is LICEF_A_21 against LICEF_B_21.
 - Next 528 rows with calibrated visibilities of elements in arm A in H polarisation against elements in arm C in V polarisation. Same order as above, i.e. first LICEF_AB_03 against LICEF_CA_03, then LICEF_AB_03 against LICEF_CA_01_V, then LICEF_AB_03 against LICEF_C_01, until the 23rd element LICEF_AB_03 against LICEF_C_21. Next is LICEF_AB_01_H against LICEF_CA_03, then LICEF_AB_01_H against LICEF_C_01, and so on until all elements in arm C are correlated with LICEF_AB_01_H (Please note that this row does not include the correlation against LICEF_CA_01_V). This ordering continues until the last element correlated is LICEF_A_21 against LICEF_C_21.
 - Next 528 rows with calibrated visibilities of elements in arm B in H polarisation against elements in arm A in V polarisation. Same order as above, i.e. first LICEF_BC_03 against LICEF_AB_03, then LICEF_BC_03 against LICEF_AB_01_V, then LICEF_BC_03 against LICEF_A_01, until the 23rd element LICEF_BC_03 against LICEF_A_21. Next is LICEF_BC_01_H against LICEF_AB_03, then LICEF_BC_01_H against LICEF_A_01, and so on until all elements in arm A are correlated with LICEF_BC_01_H (Please note that this row does not include the correlation against LICEF_AB_01_V). This ordering continues until the last element correlated is LICEF_B_21 against LICEF_A_21.

- Next 528 rows with calibrated visibilities of elements in arm B in H polarisation against elements in arm C in V polarisation. Same order as above, i.e. first LICEF_BC_03 against LICEF_CA_03, then LICEF_BC_03 against LICEF_CA_01_V, then LICEF_BC_03 against LICEF_C_01, until the 23rd element LICEF_BC_03 against LICEF_C_21. Next is LICEF_BC_01_H against LICEF_CA_03, then LICEF_BC_01_H against LICEF_C_01, and so on until all elements in arm C are correlated with LICEF_BC_01_H (Please note that this row does not include the correlation against LICEF_CA_01_V). This ordering continues until the last element correlated is LICEF_B_21 against LICEF_C_21.
- Next 528 rows with calibrated visibilities of elements in arm C in H polarisation against elements in arm A in V polarisation. Same order as above, i.e. first LICEF_CA_03 against LICEF_AB_03, then LICEF_CA_03 against LICEF_AB_01_V, then LICEF_CA_03 against LICEF_A_01, until the 23rd element LICEF_CA_03 against LICEF_A_21. Next is LICEF_CA_01_H against LICEF_AB_03, then LICEF_CA_01_H against LICEF_A_01, and so on until all elements in arm A are correlated with LICEF_CA_01_H (Please note that this row does not include the correlation against LICEF_AB_01_V). This ordering continues until the last element correlated is LICEF_C_21 against LICEF_A_21.
- Next 528 rows with calibrated visibilities of elements in Arm C in H polarisation against elements in Arm B in V polarisation. Same order as above, i.e. first LICEF_CA_03 against LICEF_BC_03, then LICEF_CA_03 against LICEF_BC_01_V, then LICEF_CA_03 against LICEF_B_01, until the 23rd element LICEF_CA_03 against LICEF_B_21. Next is LICEF_CA_01_H against LICEF_BC_03, then LICEF_CA_01_H against LICEF_B_01, and so on until all elements in arm B are correlated with LICEF_CA_01_H (Please note that this row does not include the correlation against LICEF_BC_01_V). This ordering continues until the last element correlated is LICEF_C_21 against LICEF_B_21.
- Next 23 rows with calibrated visibilities of LICEF_AB_01_H against all other receivers in arm A in V polarisation. I.e. LICEF_AB_01_H against LICEF_AB_03, LICEF_AB_01_H against LICEF_AB_01_V, LICEF_AB_01_H against LICEF_A_01, etc... until LICEF_AB_01_H against LICEF_A_21
- Next 22 rows with calibrated visibilities of all receivers in arm A in H polarisation against LICEF_AB_01_V, excluding LICEF_AB_01_H against LICEF_AB_01_V, whose equation is presented in the point above. I.e. LICEF_AB_03 against LICEF_AB_01_V, LICEF_A_01 against LICEF_AB_01_V, etc... until LICEF_A_21 against LICEF_AB_01_V
- Next 23 rows with calibrated visibilities of LICEF_BC_01_H against all other receivers in arm B in V polarisation. I.e. LICEF_BC_01_H against LICEF_BC_03, LICEF_BC_01_H against LICEF_BC_01_V, LICEF_BC_01_H against LICEF_B_01, etc... until LICEF_BC_01_H against LICEF_B_21
- Next 22 rows with calibrated visibilities of all receivers in arm B in H polarisation against LICEF_BC_01_V, excluding LICEF_BC_01_H against LICEF_BC_01_V, whose equation is presented in the point above. I.e. LICEF_BC_03 against LICEF_BC_01_V, LICEF_B_01 against LICEF_BC_01_V, etc... until LICEF_B_21 against LICEF_BC_01_V

- Next 23 rows with calibrated visibilities of LICEF_CA_01_H against all other receivers in arm C in V polarisation. I.e. LICEF_CA_01_H against LICEF_CA_03, LICEF_CA_01_H against LICEF_CA_01_V, LICEF_CA_01_H against LICEF_C_01, etc... until LICEF_CA_01_H against LICEF_C_21
- Next 22 rows with calibrated visibilities of all receivers in arm C in H polarisation against LICEF_CA_01_V, excluding LICEF_CA_01_H against LICEF_CA_01_V, whose equation is presented in the point above. I.e. LICEF_CA_03 against LICEF_CA_01_V, LICEF_C_01 against LICEF_CA_01_V, etc... until LICEF_C_21 against LICEF_CA_01_V

The following and last 3303 rows shall correspond to the imaginary values of the HV polarisation calibrated visibilities as received from the L1a products, and ordered in the approach that has been just described.

Columns in the G -matrix are generated from particularising the general equation for a certain pair of coordinates in the antenna frame (ξ - η indexes) and polarisation values of the antenna patterns and Brightness Temperature (p , q indexes).

The order of the columns shall be the following:

- The first 128x128 columns shall correspond to H polarisation Brightness Temperatures
- The next 128x128 columns shall correspond to V polarisation Brightness Temperatures
- The next 128x128 columns shall correspond to the real components of the HV polarisation Brightness Temperatures
- The final 128x128 columns shall correspond to the imaginary components of the HV polarisation Brightness Temperatures

Going into more detail, each distribution of 128x128 elements shall correspond to the SMOS natural hexagonal grid represented in a rectangular matrix. The centre (0,0) shall be the first element of the distribution. The following figures show the resulting ξ - η distribution of values for a 128x128 Brightness Temperature scene using steering 30° of MIRAS instrument:

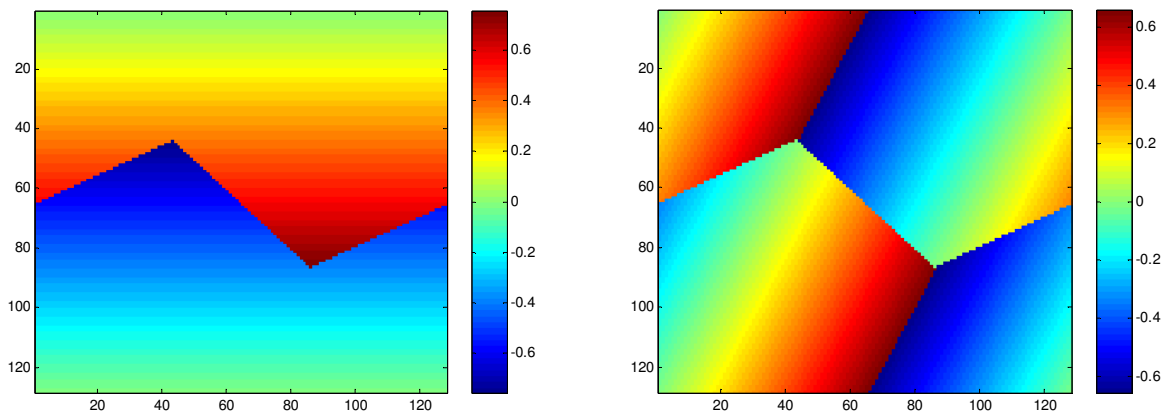


Figure 3: ξ (left image) and η (right image) coordinates proposed for the G-matrix format

The ordering of the antenna patterns should follow the one shown in the following image:

| | | | | | | | |
|--|---|-----------------------------------|-----------------------------------|--|---|---|---|
| VIS H pol 2346 complex elements +3 real elements | = | $(C^H \cdot C^{H*} \cdot R)_{re}$ | $(X^H \cdot X^{H*} \cdot R)_{re}$ | $[(C^H \cdot X^{H*} + X^{H*} \cdot C^H) \cdot R]_{re}$ | $-[(C^H \cdot X^{H*} - X^{H*} \cdot C^H) \cdot R]_{im}$ | X | BT-Trec H pol 128x128 real elements |
| | | $(C^H \cdot C^{H*} \cdot R)_{im}$ | $(X^H \cdot X^{H*} \cdot R)_{im}$ | $[(C^H \cdot X^{H*} + X^{H*} \cdot C^H) \cdot R]_{im}$ | $[(C^H \cdot X^{H*} - X^{H*} \cdot C^H) \cdot R]_{re}$ | | BT-Trec V pol 128x128 real elements |
| VIS V pol 2346 complex elements +3 real elements | = | $(X^V \cdot X^{V*} \cdot R)_{re}$ | $(C^V \cdot C^{V*} \cdot R)_{re}$ | $[(X^V \cdot C^{V*} + C^{V*} \cdot X^V) \cdot R]_{re}$ | $-[(X^V \cdot C^{V*} - C^{V*} \cdot X^V) \cdot R]_{im}$ | X | BT HV pol 128x128 complex elements |
| | | $(X^V \cdot X^{V*} \cdot R)_{im}$ | $(C^V \cdot C^{V*} \cdot R)_{im}$ | $[(X^V \cdot C^{V*} + C^{V*} \cdot X^V) \cdot R]_{im}$ | $[(X^V \cdot C^{V*} - C^{V*} \cdot X^V) \cdot R]_{re}$ | | |
| VIS HV pol 3303 complex elements | = | $(C^H \cdot X^{V*} \cdot R)_{re}$ | $(X^H \cdot C^{V*} \cdot R)_{re}$ | $[(C^H \cdot C^{V*} + X^H \cdot X^{V*}) \cdot R]_{re}$ | $-[(C^H \cdot C^{V*} - X^H \cdot X^{V*}) \cdot R]_{im}$ | X | |
| | | $(C^H \cdot X^{V*} \cdot R)_{im}$ | $(X^H \cdot C^{V*} \cdot R)_{im}$ | $[(C^H \cdot C^{V*} + X^H \cdot X^{V*}) \cdot R]_{im}$ | $[(C^H \cdot C^{V*} - X^H \cdot X^{V*}) \cdot R]_{re}$ | | |

Figure 4: G-matrix Decomposition. C and X are co- and cross-polar Antenna Patterns and R is the Fringe Wash Function multiplied by the complex exponential term (see Eq. 5)

If the level of the cross-polarisation patterns is negligible when compared to the co-polar patterns (to be addressed in a foreseen study), then the above G-matrix may be split into three independent G-matrices, each one related to one polarisation only. The format of the H and V polarisation G-matrix shall be the same, while the HV G-matrix shall be a bit bigger as shown above.

The fringe washing function will be calibrated in orbit for several baselines (those sharing noise sources), and it shall be estimated for the rest of baselines. Again, depending on the image reconstruction method, the FWF calibration shall be applied differently.

3.1.2. On-ground characterised G-matrix

This G-matrix is built based solely on input data available, such as calibration data and auxiliary data files. This method has been already implemented in SEPS, and was developed by the *Universitat Politècnica de Catalunya*. In order to calculate the G-matrix the following equation is used:

$$G(\mathbf{u};\mathbf{x}) = \frac{\hat{F}_k(\xi)\hat{F}_j^*(\xi)}{\zeta(\xi)\sqrt{\Omega_{j_1}\Omega_{j_2}}}\hat{r}_{kj}(-\Delta t)e^{-j2\pi f_0\Delta t}d\xi \tag{Eq. 5}$$

As we can see using this equation it is possible to calculate all the matrix elements using the Fringe Wash Function, \hat{r} , Antenna Patterns, \hat{F} , the solid angle of the antennas, Ω , and the spatial and frequency coordinates (\mathbf{u}, ξ).

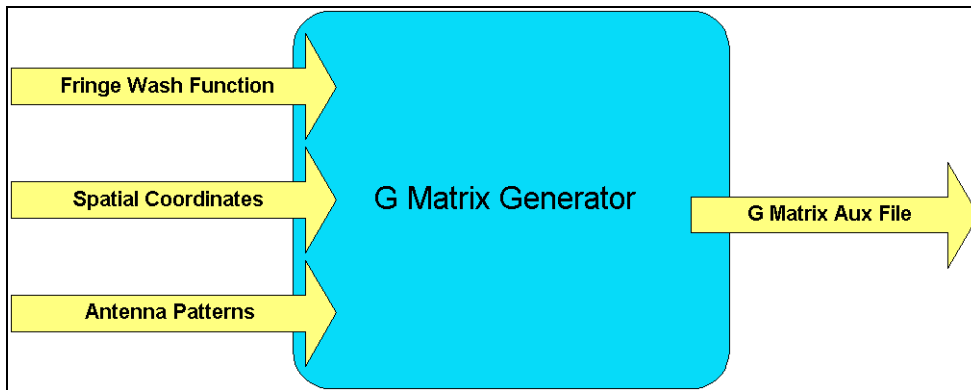


Figure 5: G-matrix Processor

3.1.2.1. Antenna Patterns

Antenna patterns shall be measured once on the ground, and a static Auxiliary Data File shall be generated with the measurements. These measurements shall be done at three different frequencies: the central operation frequency and another two at plus and minus a B bandwidth. Their use in the G-matrix construction shall be done through the pattern of the central frequency², f_0 .

As per [RD.3] the Antenna Patterns for the hinges outside the hub should be replaced by their neighbours.

| Original Hinge | Hinge to use as replacement |
|----------------|-----------------------------|
| A_09 | A_08 |
| A_10 | A_11 |
| A_15 | A_14 |
| A_16 | A_17 |
| B_09 | B_08 |
| B_10 | B_11 |

² Previously, until V5R, the baseline was to have a weighted average of the patterns at three frequencies. This has been abandoned and the current baseline is to use the central frequency only.

| | |
|------|------|
| B_15 | B_14 |
| B_16 | B_17 |
| C_09 | C_08 |
| C_10 | C_11 |
| C_15 | C_14 |
| C_16 | C_17 |

Table 3: Elements with Antenna Patterns to be replaced

Furthermore, the ESLs have shown that the best reconstruction results are obtained using an antenna pattern that is the average of the three frequencies measured, instead of using a unique frequency out of the available ones. After the average, it is necessary to perform a renormalization of each antenna pattern and the coefficients for that renormalization are provided in [RD.4].

3.1.2.2. Fringe Wash Function

The Fringe Washing Function shape shall be calibrated/estimated as part of the nominal calibration campaign, by injecting correlated noise and introducing time lags in the correlated signals. An L1a product file shall be generated every time this type of calibration is performed.

$$\hat{r}_j(\tau) \approx A \cdot \text{sinc}(B \cdot (\tau - C)) \cdot e^{i(D\tau^2 + E\tau + F)} \quad \text{Eq. 6}$$

The way to compute the different coefficients is shown in [AD.11]. The equations to be used are:

$$\begin{aligned} |g_j(-T_s)| &\approx A \cdot \text{sinc}(B \cdot (-T_s - C)) \\ |g_j(0)| &\approx A \cdot \text{sinc}(B \cdot C) \\ |g_j(+T_s)| &\approx A \cdot \text{sinc}(B \cdot (T_s - C)) \end{aligned} \quad \text{Eq. 7}$$

$$\begin{aligned} D^{H,V} &= \left(\frac{\arg(g_j^{H,V}(+T_s)) + \arg(g_j^{H,V}(-T_s))}{2} - \arg(g_j^{H,V}(0)) \right) \frac{1}{T_s^2} \\ E^{H,V} &= \frac{\arg(g_j^{H,V}(+T_s)) - \arg(g_j^{H,V}(-T_s))}{2} \frac{1}{T_s} \\ F^{H,V} &= \arg(g_j^{H,V}(0)) \end{aligned} \quad \text{Eq. 8}$$

The FWF is measured independently for the paths of the in-phase and quadrature signals, meaning that for the same visibility, there shall be two different values of the FWF. One is applicable to the real part component of the visibility, while the other is applicable to the imaginary part of the component. The following equation shows this behaviour in detail:

$$\frac{\text{Re}}{\text{Im}}\{G_j(\xi)\} = \frac{\text{Re}}{\text{Im}} \left\{ \frac{\hat{F}_{j_1}^{p_1q_1}(\xi) \hat{F}_{j_2}^{p_2q_2^*}(\xi)}{\zeta(\xi) \sqrt{\Omega_k \Omega_j}} \left\{ \begin{matrix} \hat{r}_{k,i_j}(-\Delta t_j) \\ \hat{r}_{q_k,i_j}(-\Delta t_j) \end{matrix} \right\} e^{-j2\pi f_0 \Delta t_j} d\xi \right\} \quad \text{Eq. 9}$$

It has to be remarked that the FWF shape is used in the G -matrix computation is normalised with the FWF at the origin. This means for example that the final application of the A and F coefficients will change slightly from what has been explained in the previous equations.

3.1.2.3. LICEF Spatial Coordinates

The LICEF coordinates are used to compute the applicable (u, v) baselines as per Eq. 4 can be taken from their initial measured positions in an Auxiliary Data File, or an elastic model may be applied to obtain them as a function of time. Regardless of the approach, UPC has already modelled deviations or errors in the receivers' positions as an error in the retrieved Brightness Temperatures.

3.1.3. Expanded Hexagonal Domain in the G -matrix

It is possible to use an alternative to the default size of 128x128 to characterize the (ξ, η) grid used in the definition of the G -matrix. Instead of using the regular (ξ, η) grid represented by *Figure 3* it is possible to define the grid as in Eq. 4 but with different resolution so that the Unit-Circle is circumscribed by a hexagon, i.e., with $N_T = 196$. This (ξ, η) grid is represented in *Figure 6* with the green circles, along with the other grids used in L1PP.

The impact of this modification of the grid resolution is that the size of the G -matrix changes from 4x128x128 (65536) to 4x196x196 (153664) columns, yielding an increase of the G -matrix size from ~8 GiB to ~20GiB.

All the other steps in the computation of the G -matrix are the same as described previously.

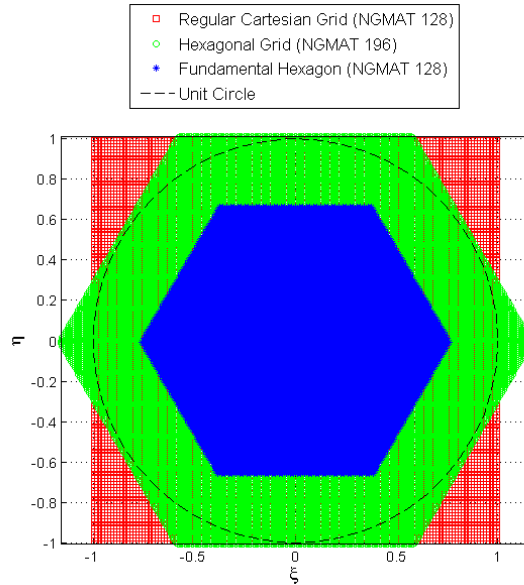


Figure 6: (ξ, η) Grids used in L1PP

3.1.4. System Response Function Mathematical Inversion

The mathematical inversion of the G -matrix is based on a band-limited regularisation, which is equivalent to:

$$\begin{cases} \min_{T \in \mathbb{R}^n} \|V - GT\|^2 \\ (I - P_H)T = 0 \end{cases} \quad \text{Eq. 10}$$

where P_H plays the role of a regularisation parameter.

This method consists in a reduction of the domain applicability, by creating the J -matrix. The G -matrix operates between Calibrated Visibilities and Brightness Temperatures, whereas the J Matrix operates between Calibrated Visibilities and Brightness Temperature Frequencies \hat{T} .

Secondly, the J -matrix is mathematically inverted using a minimum norm approach, so that the Brightness Temperature Frequencies may be obtained after a simple matrix-vector multiplication ($J^{-1} * V$)

3.1.5. Implementation

As it was described before, the G -matrix is used in two processing units, in the G -matrix multiplication unit, to generate the Delta Visibilities from the calculated temperatures, and for the J -matrix generation.

To generate the G -matrix, the L1 processor follows the processing steps described in the next diagram.

The first step is to compute the spatial coordinates, where the result will be the 128×128 (ξ, η) coordinates. These coordinates are different depending on the G -matrix type. If it is G -matrix used for the Delta Visibilities (UNIT_CIRCLE), the (ξ, η) coordinates are calculated on $N \times N$ square grid,

defined in the $[-1,1] \times [-1,1]$ domain. In case of the G -matrix used for J -matrix computation (HEXAGON) the (ξ, η) coordinates are calculated based on a different approach. The configurable option to use the expanded hexagonal G -matrix (HEXAGON_UNIT_CIRCLE) triggers the computation of the (ξ, η) as an hexagonal grid defined with Eq. 4 and with $N_T = 196$.

After the (ξ, η) coordinates calculations, the antenna patterns are computed using the Eq. 6, to get the weighted average measurements. In this step the measurements from the 181x181 grid are interpolated to the 128x128 grid, using the (ξ, η) coordinates. The interpolation is performed doing a running average on the 181x181 amplitude and phase values.

The following step is the computation of the Fringe Wash Function shape according to the Eqs. 6, 7 and 8.

Finally, after all the previous steps we apply the Eq. 5 to generate the on-ground characterised G -matrix and to produce an Auxiliary Data File for the Delta Visibilities G -matrix or a temporary file for the J -matrix generation. For each pair of receivers, the LICEF coordinates are loaded into memory and u , v and w are calculated using Eq. 3.

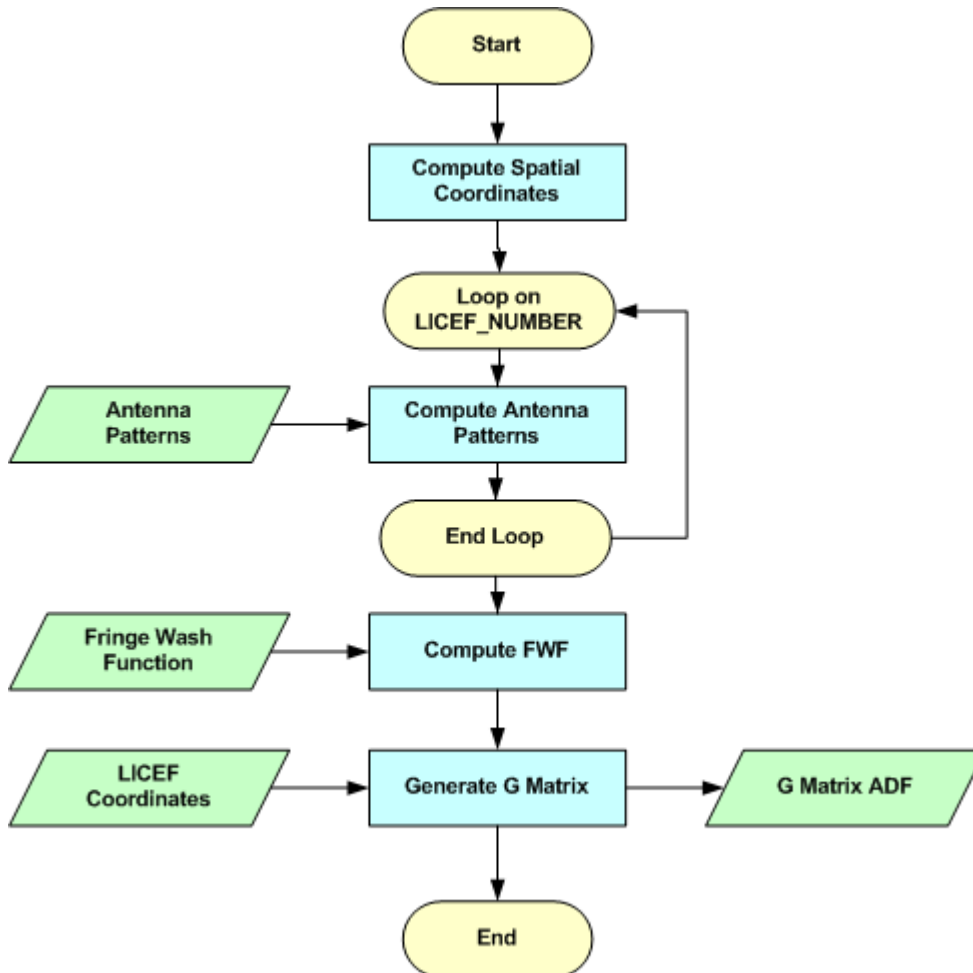


Figure 7: On-ground characterised G-matrix Generation

3.1.5.1. Inputs

- Auxiliary file with antenna amplitude and phase patterns (SM_xxxx_AUX_PATT##_<ID>).
- Auxiliary file with Weights per frequency and Normalization factors per LICEF (SM_xxxx_AUX_PLM__<ID>).
- Auxiliary file with LICEF positions (SM_xxxx_AUX_PLM__<ID>).
- L1a Fringe Wash Function File with the estimated coefficients used in the computation of the G-matrix (SM_xxxx_MIR_FWAS1A<ID>).

3.1.5.2. Outputs

- G-matrix auxiliary file to be used in the Foreign Sources Correction and Image Reconstruction Process (SM_xxxx_AUX_GMAT__<ID>).

3.1.5.3. List of Variables

The following table describes the variables used in the subsequent implementation section. Variables are listed as input, local and output (I, L, O). The *Size* column indicates the number of elements constituting that variable, and NOT the size of the variable in bytes (this information can be taken from the *Type* column).

| Variable name | Description | Definition | Type | Class | Unit | Size |
|---------------------------|--|------------|------|-------|------|---------|
| fwf_filename | Fringe Wash Function ADF. | N/A | char | I | N/A | Pointer |
| antenna_patterns_filename | Antenna Patterns ADF filename | N/A | char | I | N/A | Pointer |
| ap_correction_factors | Weights to apply to each Frequency and Normalization factors | N/A | | I | N/A | Pointer |
| antenna_patterns | Antenna Patterns | N/A | | L | | |
| fwf_corrected | Fringe Wash function computed | Eq. 8 | | L | N/A | |
| spatial_coordinates | Spatial coordinates computed | Eq. 4 | | L | | |

| Variable name | Description | Definition | Type | Class | Unit | Size |
|---------------|----------------|------------|--------|-------|------|-------------------------|
| gmatrix | G-matrix data. | Eq. 5 | double | O | N/A | [15996] x [65536] |

Table 4: On-ground characterised G-matrix Variable List

3.1.5.4. Implementation details

The function *generate_gmatrix* is presented below. It represents a first approach with the methods needed to generate the on-ground characterised G-matrix.

First the (ξ, η) coordinates matrices are generated. These matrices are different depending on the G-matrix type. If it is the “HEXAGON” the function *computeCoordinates* will be the following:

```

for (i=0;i!=N;++i){
    for (j=0;j!=N;++j){
        if (i > j){
            ii = i-N; jj = j;
            if ((2*i+j-N) < 0){ ii = i;    jj = j;}
            if ((i+2*j-2*N) > 0){ ii = i-N; jj = j-N;}
        }else{
            ii = i; jj = j-N;
            if ((i+2*j-N) <= 0){ ii = i;    jj = j;}
            if ((2*i+j-2*N) >= 0){ ii = i-N; jj = j-N;}
        }
        eta[i][j] = (jj + 0.5 * (float) ii) / (N * d * (sqrt(3) / 2));
        xi[i][j] = (0.5 * sqrt(3) * (float) ii) / (N * d * (sqrt(3) / 2));
    }
}

```

with $N = 128$. For the HEXAGON_UNIT_CIRCLE G-matrix, the function used to compute the (ξ, η) coordinates is the same as above, but using $N = 196$.

In the case of the “UNIT_CIRCLE” G-matrix the *computeCoordinates* function will have the following source code:

```

step = 2.0 / (N_GMAT);
for (i = 0; i < N; i++){
    for (j = 0; j < N_GMAT; j++){
        xi[i][j] = (-1 + (step/2)) + (i*step);
        eta[i][j] = (-1 + (step/2)) + (j*step);
    }
}

```

```
#define N 128
error = computeCoordinates(xi, eta);
error = computeAntennaPatterns(antenna_patterns_filename, xi, eta,
antenna_patt_corrected);
error = computeFWFshape(fwf_filename, u, v, xi, eta, fwf_coefs);
for(i=0; i!=LICEF_NUMBER; ++i){
  for(j=0; j!=LICEF_NUMBER; ++j){
    error = computeReceiverPositions(licef_coordinates_data, i, j, &u, &v, &w);
    for(int k=0; k!=N; ++k){
      for(int l=0; l!=N; ++l){
        switch(pol_mod){
          case H, V or HV:
            error = prepareFWF(pol_mode, i, j, k, l, fwf_shape, fwf_coefs);
            g_element = (1/(sqrt(1-(xi*xi)(eta*eta))))*(antenna_patt_corrected)*
(fwf_coefs)*exp(sqrt(-1)*2*PI*(u*xi+v*eta));
            error = addGelement(g_element);
          break;
        }
      }
    }
  }
}
```

The G -matrix is computed based on Eq. 5, but first the antenna patterns and the fringe wash function shape must be obtained. The LICEF coordinates must also be loaded in memory.

The *compute_antenna_patterns* needs to perform interpolation for each polarization mode on the antenna measurements, because originally the measures are stored in an 181x181 matrix and for the G -matrix computation must be 128x128 (or 196x196 for the hexagonally expanded G -matrix). This function also replaces the hinges antenna patterns by their neighbours.

compute_fwf_shape method applies Eq. 6 to get the fringe wash function shape ready to compute the G -matrix. This function will return the A, B, C, D, E, and F Fringe Wash Function coefficients needed to compute each value of the G -matrix, depending on polarization mode. The method receives an

averaged Fringe Wash Function product and extracts the coefficients A, B, C, D and E. F is not needed, and can be set to zero, as the FWF shape used in the G -matrix generation is normalised.

The phase coefficients D, E and F are obtained immediately for each baseline by simply applying Eq. 8. The magnitude coefficients must be computed using a Newton-Raphson method by approximating the values in Eq. 7 to a sinc function. The implementation is shown below for each baseline k :

```
/* FWF values at +T and -T must be normalized to the origin*/
fwf1_abs = fwf1_abs / fwf0_abs; //FWF at -T
fwf2_abs = fwf2_abs / fwf0_abs; //FWF at +T
/*initial solution for Newton Raphson*/
counter = 0; error = 100; //timestep is the value of +T
p1 = (fwf2_abs - fwf1_abs) * timestep / (fwf2_abs + fwf1_abs -2.);
p2 = -2. * timestep * timestep / (fwf2_abs + fwf1_abs -2.);
AII[k] = 1. + p1 * p1 / 4. / p2;
BII[k] = sqrt(6. / AII[k] / p2) / PI;
CII[k] = -p1 / 2.;
/*avoid singularities when fwf2_phase = fwf1_phase*/
if (fabs(fwf2_abs - fwf1_abs) > eps)
{
    solution[0] = PI * BII[k] * timestep;
    solution[1] = PI * BII[k] * CII[k];
    while (fabs(error) > eps && counter < 100)
    {
        vector[0] = (fwf1_abs * (solution[0] + solution[1]) * sin(solution[1])) - solution[1]
* sin(solution[0] + solution[1]);
        vector[1] = (fwf2_abs * (-solution[0] + solution[1]) * sin(solution[1])) -
solution[1] * sin(-solution[0] + solution[1]);
        jacobian[0] = fwf1_abs * sin(solution[1]) - solution[1] * cos(solution[0] +
solution[1]);
        jacobian[2] = fwf1_abs * sin(solution[1]) + fwf1_abs * (solution[0] + solution[1]) *
cos(solution[1]) - (sin(solution[0] + solution[1]) + solution[1] * cos(solution[0] +
solution[1]));
        jacobian[1] = -fwf2_abs * sin(solution[1]) + solution[1] * cos(-solution[0] +
solution[1]);
        jacobian[3] = fwf2_abs * sin(solution[1]) + fwf2_abs * (-solution[0] + solution[1]) *
cos(solution[1]) - (sin(-solution[0] + solution[1]) + solution[1] * cos(-solution[0] +
solution[1]));
        dgesv_(&n, &nrhs, jacobian, &n, ipiv, vector, &n, &info);
        solution[0] -= vector[0];
        solution[1] -= vector[1];
        error = vector[0]*vector[0] + vector[1]*vector[1];
        counter++;
    }
    BII[k] = solution[0] / timestep / PI;
    AII[k] = 1. / sinc(-solution[1] / PI);
}
```

In the specific case that the magnitude of FWF at +T and -T are exactly equal, the above resolution cannot be performed, so another approximation must be implemented.

```
else /*singular case where fwf2_abs = fwf1_abs, cannot use Newton Raphson*/
{
    solution[0] = PI * BII[k] * timestep;
    while (fabs(error) > eps && counter < 100)
    {
        vector[0] = fwf1_abs * solution[0] - sin(solution[0]);
        jacobian[0] = fwf1_abs - cos(solution[0]);
        solution[0] -= (vector[0]/jacobian[0]);
        error = vector[0]/jacobian[0];
        counter++;
    }
    BII[k] = solution[0] / timestep / PI;
    AII[k] = 1.;
    CII[k] = 0.;
}
```

With this code, the FWF shape amplitude coefficients are computed normalised to the FWF value at the origin.

For each pair of LICEFs the receiver positions must be calculated using Eq. 3, the function responsible for these calculations is *computeReceiverPositions* and returns the values of the (u,v,w) -coordinates generating the visibility sample V_j .

The G -matrix element is calculated using Eq. 9 where the real part uses the fringe wash function shape \hat{r}_{ikj} and the imaginary part uses the function shape \hat{r}_{qkij} . At this point the two antenna patterns that build up the (k, j) baseline being processed are averaged according to the weights specified and renormalized with the correction factors provided in [RD.4].

The method *add_g_element* will add the elements to the G -matrix and each value will be stored as double. The real part for each polarization mode is stored in the first 2346 lines and the imaginary in the next 2346. With this approach the future operations are easier to implement since the real part is already separated from the imaginary part. In the HV part there will be two columns, one with the real part and other with the imaginary and instead of 2346 lines there will be 3303.

The row order used in the G -matrix generation is described in a previous section of the document (Section 3.1).

The resulting G -matrix must be order by 4x128x128 columns (corresponding to the (ξ, η) coordinates) and 15996 lines (corresponding to the pairs of LICEFs).

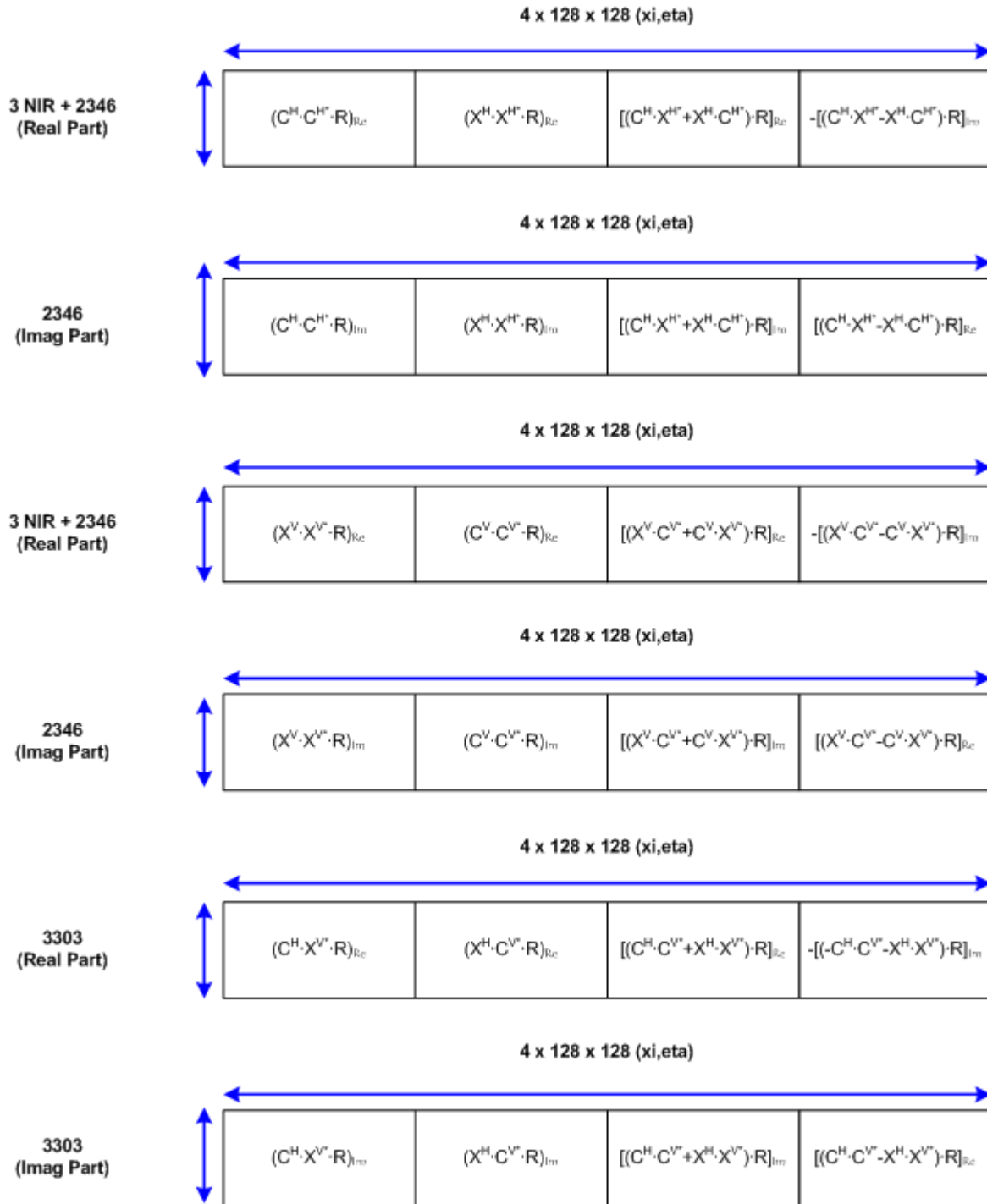


Figure 8: G-matrix Order (see also Figure 4)

In the previous figure it is demonstrated how the G-matrix lines and columns are ordered. If the type of G-matrix being generated is HEXAGON_UNIT_CIRCLE, then in **Figure 8** and the in the last paragraphs, the 128 should be replaced by 196

For the NIR receivers the Fringe Wash Function shape is not needed. The real part of Fringe Wash is 1 and the imaginary 0, since there is no correlation between receivers.

In order to simplify the calculations, the number of columns and rows of the G -matrix are different if it is considered dual or full polarization. In the case of dual polarization the G -matrix actually consists of a pair of blocks, one for each polarization, with 4695 rows by 32768 (for $N_T = 128$ and 76832 for $N_T = 196$) columns per block. Compared with the full polarization, the vector matrix product is a quicker process since the matrix is smaller.

It is very important to store in the G -matrix header the correlator layer (Nominal or Redundant) that was active when the FWF shape was measured. This value can be retrieved from the FWF shape product header, and it is required in order to determine which data can be reconstructed with the G -matrix product.

3.2. AUX_JMAT

This matrix represents the mathematical reduction of the previous G -matrix in order to obtain Brightness Temperatures frequencies. It represents the System Response Function of the instrument transforming Calibrated Visibilities plus the zero frequency value measured through the NIR elements into Brightness Temperature Frequencies.

This is the matrix that shall be inverted to complete the Image Reconstruction process. Regardless of how the G -matrix is built, the size of the Brightness Temperature grid, or what modelling it has used, its reduction into the J -matrix shall always have the same format and size.

The number of columns is now dependent on the (u,v) frequency domain, and is restricted to the number of non-redundant correlations that the instrument shall be measuring. For MIRAS, the number of non-redundant visibilities is 2791, forming a star shape in the (u,v) plane, and is only dependent on the number of receivers per arm and the Y shape of the instrument.

Thus, the number of columns for this matrix shall be 11164. This number comes from 1395 complex elements plus one real element that is measured for H or V polarisation, plus 2791 complex elements measured for HV polarisation. Again, the total size of the matrix is dependent on the level of coupling between polarisations through the cross-polarisation antenna patterns. If they can be considered negligible, the J matrix can be split into three separate and independent matrices, one for each polarisation.

For the column elements ordering, it shall follow the ordering indicated below:

- The first column shall correspond to the real component of the zero baseline for the H polarisation Brightness Temperature frequencies
- The next 1395 columns shall correspond to the real components of the H polarisation Brightness Temperature frequencies
- The next 1395 columns shall correspond to the imaginary components of the H polarisation Brightness Temperature frequencies

- ❑ The next column shall correspond to the real component of the zero baseline for the V polarisation Brightness Temperature frequencies
- ❑ The next 1395 columns shall correspond to the real components of the V polarisation Brightness Temperature frequencies
- ❑ The next 1395 columns shall correspond to the imaginary components of the V polarisation Brightness Temperature frequencies
- ❑ The next 2791 columns shall correspond to the real components of the HV polarisation Brightness Temperature frequencies, with the zero baseline as the first column

The next 2791 columns shall correspond to the imaginary components of the HV polarisation Brightness Temperature frequencies, with the zero baseline as the first column.

The distribution of elements within each sub-group of 1395 columns shall follow the order described next. This ordering is based on reporting only the baselines with positive v coordinate and u positive for $v=0$:

- ❑ The v coordinate for the upper half of the baselines goes continuously from 0 to $\sqrt{3} \cdot \text{NEL} \cdot d$, where $\text{NEL}=21$ and $d=0.875$, in incremental steps of $\sqrt{3} \cdot d/2$
- ❑ The u coordinate of the upper half of the baselines shall follow the mathematical rules defined as:
 - If $v=0$, then u goes from d to $24 \cdot d$ in incremental steps of d
 - If $v>0$ and $v \leq \sqrt{3} \cdot \text{NEL} \cdot d/2$, then u goes from $-(\text{NEL} \cdot d + v/\sqrt{3})$ to $+(\text{NEL} \cdot d + v/\sqrt{3})$ in incremental steps of d
 - If $v = \sqrt{3} \cdot (\text{NEL} + 1) \cdot d/2$, then u goes from $-11 \cdot d$ to $+11 \cdot d$ in incremental steps of d
 - If $v = \sqrt{3} \cdot (\text{NEL} + 2) \cdot d/2$, then u has the values $-23 \cdot d/2$, $-19 \cdot d/2$ to $+19 \cdot d/2$ in incremental steps of d and $+23 \cdot d/2$. Notice that the elements $\pm 21 \cdot d/2$ are not present.
 - If $v = \sqrt{3} \cdot (\text{NEL} + 3) \cdot d/2$, then u has the values $-12 \cdot d$, $-9 \cdot d$ to $+9 \cdot d$ in incremental steps of d and $+12 \cdot d$. Notice that the elements $\pm 11 \cdot d$ and $\pm 10 \cdot d$ are not present.
 - Finally, if $v > \sqrt{3} \cdot (\text{NEL} + 3) \cdot d/2$ and $v \leq \sqrt{3} \cdot \text{NEL} \cdot d$, then u goes from $-(\text{NEL} \cdot d - v/\sqrt{3})$ to $+(\text{NEL} \cdot d - v/\sqrt{3})$ in incremental steps of d

The order followed is shown in the next picture. For the 1395 element vector, the baselines shall be taken first from left to right, then from bottom to top. I.e. the first 24 elements are the ones with $v=0$ and ordered by increasing u ; the next 42 elements are the ones with $v = \sqrt{3} \cdot d/2$ and ordered by increasing u (from negative to positive), and so on until the 1395 elements are covered.

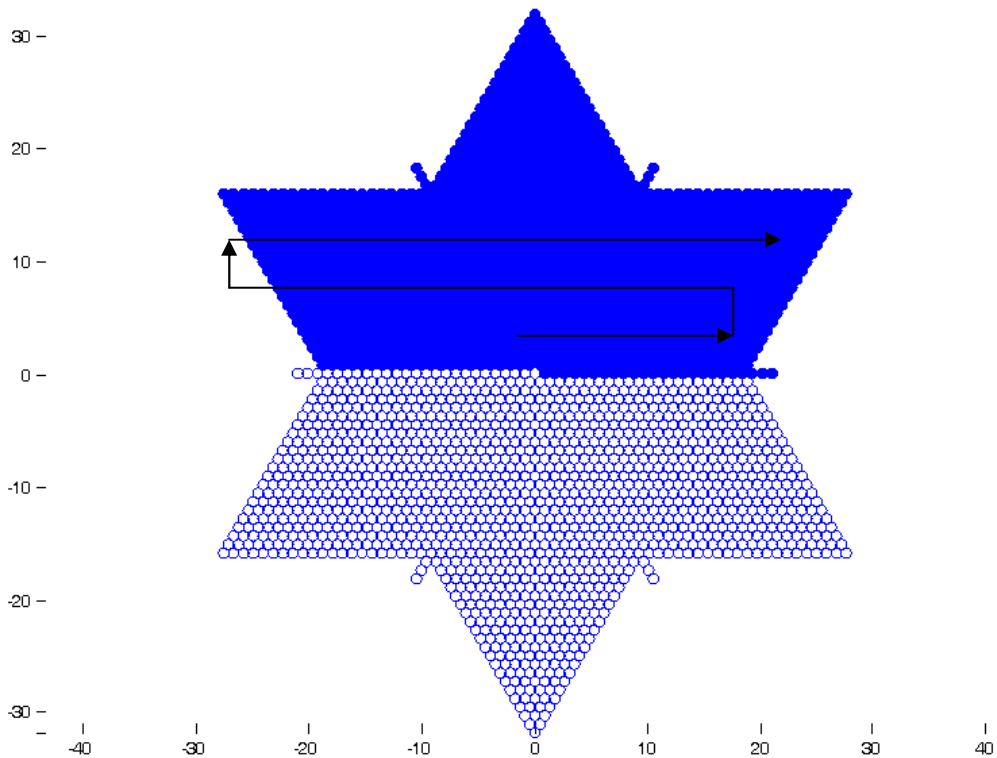


Figure 9: J Matrix Representation

For the case of HV polarisation, where the vector is 2791 elements long, the complete star must be covered. In this case, the ordering shall be similar to the one adopted above. The first element shall be the zero baseline ($u=0, v=0$); the next 1395 elements shall be ordered like it has been described (left to right, then bottom to top); and the remaining 1395 element shall be ordered in the same way as well, but inverting the sign of the resulting u and v coordinates (i.e. it changes to ordering from right to left, then top to bottom).

The resulting J matrix shall be inverted, making it possible to obtain the Brightness Temperature frequencies by simple multiplication of the inverted J by the L1a calibrated visibilities. It is important to define a common format so that the L1b output is coherent.

3.2.1. J Matrix Inversion

Once it has been generated, the J -matrix needs to be inverted in order to obtain $\hat{T}(u, v)$. The inversion is achieved by using the pseudo-inverse:

$$\begin{aligned}
 J \cdot \hat{T} &= V \\
 J^* J \cdot \hat{T} &= J^* V \\
 \hat{T} &= (J^* J)^{-1} J^* V \\
 J^+ &= (J^* J)^{-1} J^*
 \end{aligned}
 \tag{Eq. 11}$$

J is the System Response Function expressed in the Brightness Temperatures Frequency domain (star domain). J^* is the conjugate transpose of J , and J^+ is its pseudo-inverse

The result of multiplying J^+ by the calibrated visibilities V is the brightness temperatures frequencies $\hat{T}(u, v)$, expressed in the frequency star domain.

In fact, in order to give the user more configuration flexibility to take into account e.g. possible hardware failures, the temperature frequencies are instead obtained by multiplying J^+ by WV ($\hat{T} = J^+ WV$), where W is a diagonal matrix whose entries consist of user configurable weights for each baseline. These baseline weights (whose default value is 1) are obtained from the SM_XXXX_AUX_BWGHT_<ID> Auxiliary Data File defined in [AD.13].

As a further step for the baseline weighting, the method described in [RD.6] is recommended for the operational algorithm. This method consists on a baseline avoidance algorithm, which will respect the format of the J^+ matrix, but will take into account during the inversion process that some baselines are not desired (i.e. NIR-NIR baselines across arms and baselines across instrument hinges). This algorithm will use data from two additional auxiliary files during the J matrix inversion (BWGHT and FAIL ADF).

The baselines identified as the ones to be always removed are:

| NIR-NIR baselines | | Hinges baselines | |
|-------------------|-----------------------------|------------------|-------------------|
| 01 | NIR-AB-01 H --- NIR-BC-01 H | 1 | LCF-A-03 LCF-A-04 |
| 02 | NIR-AB-01 H --- NIR-BC-01 V | 2 | LCF-A-09 LCF-A-10 |
| 03 | NIR-AB-01 H --- NIR-CA-01 H | 3 | LCF-A-15 LCF-A-16 |
| 04 | NIR-AB-01 H --- NIR-CA-01 V | 4 | LCF-B-03 LCF-B-04 |
| 05 | NIR-AB-01 V --- NIR-BC-01 H | 5 | LCF-B-09 LCF-B-10 |
| 06 | NIR-AB-01 V --- NIR-BC-01 V | 6 | LCF-B-15 LCF-B-16 |
| 07 | NIR-AB-01 V --- NIR-CA-01 H | 7 | LCF-C-03 LCF-C-04 |
| 08 | NIR-AB-01 V --- NIR-CA-01 V | 8 | LCF-C-09 LCF-C-10 |
| 09 | NIR-BC-01 H --- NIR-CA-01 H | 9 | LCF-C-15 LCF-C-16 |
| 10 | NIR-BC-01 H --- NIR-CA-01 V | | |
| 11 | NIR-BC-01 V --- NIR-CA-01 H | | |
| 12 | NIR-BC-01 V --- NIR-CA-01 V | | |

Table 5 - Baselines to be removed from J^+

3.2.2. Implementation

This method requires to compute the J -matrix, whose size is much smaller than the G , as it merely relates the calibrated visibilities to the brightness temperatures frequencies, \hat{T} . The number of these frequencies is equal to the number of non-redundant baselines N_f : 1396 for H and V polarisations and 2791 for HV polarisation.

The matrix J is computed by using G to create the expected calibrated visibilities for some specific Brightness Temperatures. These specific Brightness Temperatures are computed by setting to unity each of the non-redundant baselines in the star domain and perform a normal 2D IFFT on the resulting distribution. Each computed set of Brightness Temperatures for each of the non-redundant baselines results in a complete column of the J matrix.

The method can be modelled in the following way:

- Enter a for loop for each of the non-redundant baselines, which correspond to a particular (U, V) position (the order to be taken is described in [AD.5])
- Using Eq. 11 an $N_T \times N_T$ complex matrix is created for the u, v baselines with zero in all positions except for the (u, v) position where the complex number $(1+i)$ is set.
- In H or V polarisation, the complex number $(1-i)$ is also set in the $(-u, -v)$ position, and only half of the non-redundant baselines shall be used (1396)
- In HV polarisation no other value is changed from zero, and all the non-redundant baselines shall be used (2791)
- A 2D Inverse Fast Fourier Transform is performed on the resulting $N_T \times N_T$ complex matrix, which will generate a new $N_T \times N_T$ complex matrix. In H or V polarisation, as the input matrix is Hermitian, the output matrix shall be real valued.
- This new $N_T \times N_T$ complex matrix is ordered in vector format, zero-padded to form a $4 \times N_T \times N_T$ real valued vector and multiplied by G as shown in Figure 10. Notice that depending on the polarisation being used, the zero padding of the vector in the figure may vary (e.g. if the vector corresponds to H polarisation, the V and HV polarisation components must be filled with zeroes).
- The resulting vector of the matrix vector multiplication shall be a complete column of the J matrix applicable to the (u, v) baseline.

Continue the loop until all columns of J have been computed.

After the generation of the J -matrix it is needed to invert (J^+) it in order to be used in the image reconstruction module. To do the inversion Eq. 11 will be used and then the module will generate the corresponding ADF file.

The result of multiplying J^+ by the calibrated visibilities V is the brightness temperatures frequencies $\hat{T}(u, v)$, expressed in the frequency star domain.

The calibrated visibilities must be ordered in a very precise way, in order to match the way in which the J - and G -matrices were generated. This ordering is described in chapter 4.18.3 of [AD.5]. Visibilities for

H and V polarisations in two consecutive integration times must be used in dual polarisation mode, while visibilities for H, V and HV polarisation in two consecutive integration times must be used in full polarisation mode. For a comprehensive analysis on the HV visibilities ordering and location, please refer to [RD.2].

In addition, the new Baselines Avoidance Algorithm has been implemented in L1PP. This file takes into account baselines affected by external contamination and which are not desired in the reconstruction process, and filters them out during the inversion process. For detailed information, please refer to [RD.6].

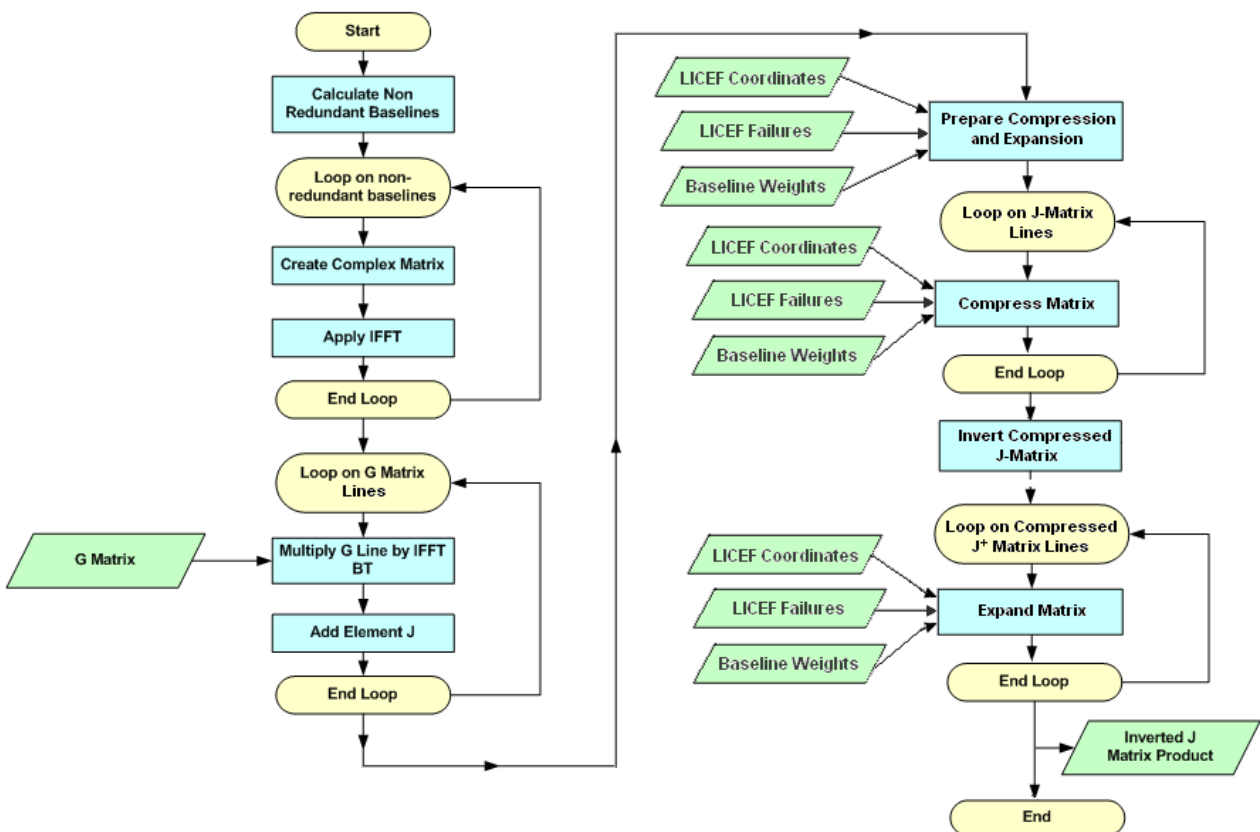


Figure 10: J-matrix Generation and Inversion Flow

3.2.2.1. Inputs

- G-matrix auxiliary file (SM_xxxx_AUX_GMAT_<ID>)
- Baseline Weights auxiliary file (SM_xxxx_AUX_BWGHT_<ID>)
- Element Failure auxiliary file (SM_xxxx_AUX_FAIL_<ID>)

3.2.2.2. Outputs

- Inverted J-matrix auxiliary file (SM_xxxx_AUX_JMAT__<ID>)

3.2.2.3. List of Variables

The following table describes the variables used in the subsequent implementation section. Variables are listed as input, local and output (I, L, O). The *Size* column indicates the number of elements constituting that variable, and NOT the size of the variable in bytes (this information can be taken from the *Type* column).

| Variable name | Description | Definition | Type | Class | Unit | Size |
|-------------------|-----------------------------|--|--------|-------|------|-------------------|
| gmatrix_filename | G-matrix ADF filename | N/A | char | I | N/A | Pointer |
| coord_matrix | Matrix ready to apply IFFT | Eq. 4 | | L | | [128] x [128] |
| coord_matrix_ifft | Recovered Matrix | N/A | real | L | | [128] x [128] |
| J_mat_column | J-matrix in vector column | | double | L | | 15996 |
| Jmatrix | Complete J-matrix | Section Error! Reference source not found. | double | L | | [15996] x [11164] |
| Jmatrix_inv | Inverted J-matrix (J^+) | Eq. 11 | double | O | N/A | [15996] x [11164] |

Table 6: J Matrix Variable List

3.2.2.4. Implementation details

The function *generate_jmatrix* is responsible for the generation of a J-matrix already inverted. It receives as input a G-matrix created before. The output will be a J-matrix already inverted and ready for the image reconstruction module.


```
error = getUVBaselines(u, v);
error = getNRBaselines(u, v, nr_baselines);
for(i=0;i!=nr_baselines.count;++i){
    error = computeCoordinates(u[i], v[i], coord_matrix_real, coord_matrix_img);
    /*Compute IFFT using fftw_plan_dft_2d function*/
    error = applyIFFT(coord_matrix, coord_matrix_ifft);
    error = multiplyIFFTGmat(gmatrix, coord_matrix_ifft, j_mat_column);
    jmatrix[0][n] = j_mat_column;
}
error=invertJmat(jmatrix, jmatrix_inv);
```

The first thing to do is to obtain the non-redundant baselines, using the (u,v) coordinates ~~and the conditions present in Section Error! Reference source not found.~~ The result will be 1395 (u,v) coordinates forming the star domain present in Figure 9.

The function starts to invoke the *compute_coordinates* method to build the complex matrix for the u and v baselines with zero in all positions except in one position (where $1+i$ is set). It is needed to set to one the position $(1-i)$, in order to produce a hermitian matrix. This will generate two 128×128 matrices, one with the real part (set to 1 and -1) and other with the imaginary part (set to i and $-i$) ready to apply the IFFT. In full polarization the entire star must be covered, then it will not be only 1395 baselines but 2791 complex values, instead of real values.

The following code presents the *getUVBaselines* function. It is implemented based on Eq. 4. It computes a rectangular matrix with the coordinates of the (u,v) distribution in the frequency domain.

```
for (i=0;i!=N-1;++i){
  for (j=0;j!=N-1;++j){
    if (i > j){
      ii = i-N; jj = j;
      if ((2*i+j-N) < 0){ ii = i;   jj = j;}
      if ((i+2*j-2*N) > 0){ ii = i-N; jj = j-N;}
    }else{
      ii = i; jj = j-N;
      if ((i+2*j-N) <= 0){ ii = i;   jj = j;}
      if ((2*i+j-2*N) >= 0){ ii = i-N; jj = j-N;}
    }
    if (i > 0){ U(j,N-i) = (jj + 0.5*ii)*d;}
    if (i == 0) U(j,i) = (jj + 0.5*ii)*d;
    V(N-j,i) = (0.5*sqrt(3)*ii)*d;
  }
}
```

The *apply_ifft* method will use the fftw library methods. At this level we will use the function `fftw_plan_dft_2d`. It receives as arguments the number of lines and columns, the source matrix and the FFT method. The type of the source and result matrix must be `fftw_complex` and the memory allocation must be done by the fftw methods. The resulting IFFT values must not be normalized.

After the IFFT vectors are calculated it is needed to transform them to a column vector to be multiplied with the *G*-matrix. The result of this operation is one column of the *J* matrix. In order to optimize the operation the method *multiply_ifft_gmat* will only load one line of the *G*-matrix and multiply it by all the ifft vectors.

```

m = gmatrix_rows; n = gmatrix_columns;
for(int i=0; i!=gmatrix_rows;++i){
    error = getGLLine(i, g_mat_line);
    //Dual Pol
    for(int j=0;j != NRB, ++j){
        j_matrix[i][j] = ddot_(&line_size, g_mat_line, &step, ifft_vector_real[j],&step);
        j_matrix[i][j+1395] = ddot_(&line_size, g_mat_line, &step, ifft_vector_imag[j],
&step);
    }
    //Full Pol
    for(int j=0;j != NRB, ++j){
        j_matrix[i][j] = ddot_(&line_size, g_mat_line, &step, ifft_vector_real[j],&step);
        j_matrix[i][j+2791] = ddot_(&line_size, g_mat_line, &step, ifft_vector_imag[j],
&step);
    }
}
    
```

The result J Matrix will have the structures presented in the picture below.

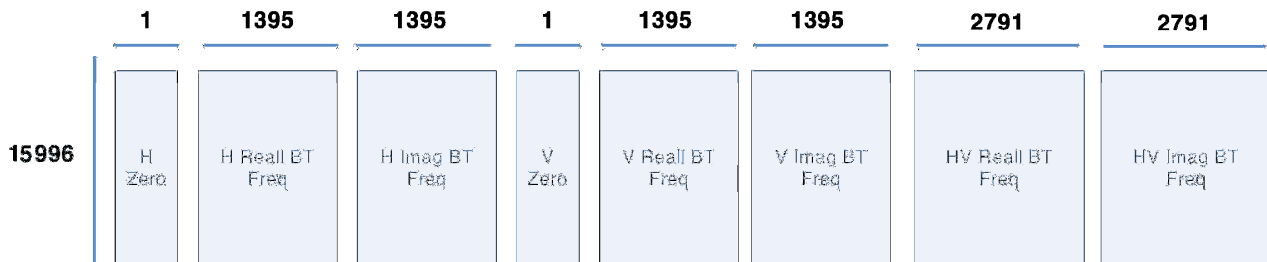


Figure 11: J Matrix Structure

The *invert_j_matrix* method uses some LAPACK methods to invert the J matrix generated. The inversion is performed using SVD methods. After the Singular Value Decomposition of J is performed ($J=UxSxV^T$), the pseudo-inverse J^+ is easily computed doing $J^+=V^T x S^{-1} x U$.

```

dgesvd(&jobu, &jobvt, &ncols, &nrows, matrix, &ldmatrix, s, u, &ldu, vt, &ldvt, work,
&lwork, &info);
for (i=0;i<ncols;i++)
    {matrix[i][i] = 1./s[i];}
dgemm(&transa, &transb, &nrows, &ncols, &nrows, &alfa, vt, &nrows, matrix, &ncols,
&beta, svd_matrix, &nrows);
dgemm(&transa, &transb, &nrows, &ncols, &ncols, &alfa, svd_matrix, &nrows, u, &ncols,
&beta, matrix, &nrows);
jmatrix_inv=matrix;
    
```

In order to confirm that the inversion values are in line with the expected it is good to check the output of the `dgesvd_` function. The rank, or number of Singular Values “significantly” different from zero, must be exactly the number of columns (2791x4). This is easily seen in a representation of the SVD values like in the next figure, by verifying that there are no magnitude jumps which could indicate duplication of lines in previous computations. This method is mentioned here because it has been a great help during the prototype implementation.

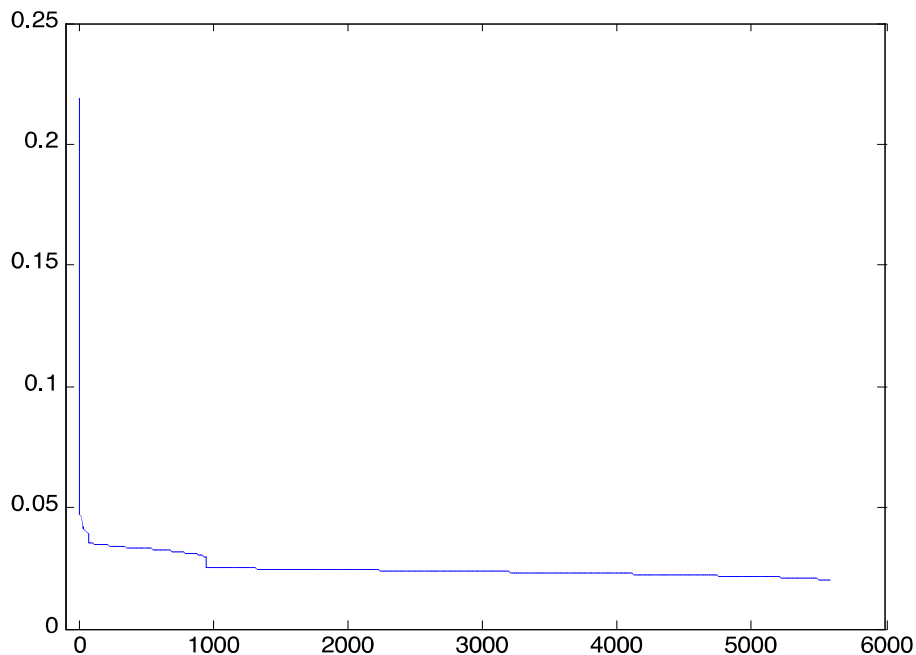


Figure 12: SVD Output Values

It is very important to store in the J^+ -matrix header the correlator layer (Nominal or Redundant) that was active when the FWF shape, used to compute the G -matrix, was measured. This value can be

retrieved from the FWF shape product header, and it is required to determine which data can be reconstructed with the J+ matrix product.

3.3. AUX_FTT

This is a specific module which generates the FTT ADF based on External Target observation data. Such generation is based on consecutive scenes taken while observing a relatively Flat portion of the Sky, and the instrument measurements together with other L1PP generated data shall be stored in the ADF for later use during nominal processing.

This module shall select a sequence of continuous external target scenes (typically 500, but value shall be configurable) whose expected Sky image RMS is lower than a certain configurable value. The RMS values shall be taken from the Galaxy Map ADF, where they have been computed beforehand.

Once the scenes are selected, this module shall perform an averaging of all the L1a calibrated visibilities, producing 3 averaged output scenes: one for H polarisation, one for V polarisation and another for HV polarisation (this last only if measuring in full pol mode, otherwise it shall be set to 0). Furthermore, according to the Baseline Based Algorithm for the Flat Target Transformation, [RD.5], this module also computes the average physical temperature for the 72 receivers.

Additionally, it shall also average the NIR Brightness Temperatures for all the scenes, and the physical temperature of the receivers.

Besides this data averaging, the processing module shall also compute additional visibilities using the best instrument modelling available (i.e. the latest *G*-matrix). One set of visibilities for the expected Sky observed, and another for a uniform 1K scene in the whole unit circle.

For this purpose it shall compute the expected Sky Brightness Temperature in the Antenna Plane being observed by the instrument during the scene averaging. This information shall be computed using the instrument pointing and the Galaxy Map BT distribution and the average value for each polarization is also stored for the computation of the scaling factors to be applied during the science processing.

The 1K scene is self-explanatory, as it shall always be 1 regardless of the ξ - η coordinates.

These two BT distributions (in all available polarisations) shall be multiplied by the *G*-matrix, obtaining the expected visibilities as output. As part of this output, the expected NIR BT shall also be obtained. As these visibilities are computed using the *G*-matrix, their sizes shall be the following ones:

- V_{SkyFFT} shall contain 3 real elements plus 2346 complex elements for H or V polarisation, and 3303 complex elements for HV polarisation
- $V_{\text{UniformFFT}}$ shall contain 3 real elements plus 2346 complex elements for H or V polarisation, and 3303 complex elements for HV polarisation

V_{FFT} shall contain 3 real elements plus 2556 complex elements for H or V polarisation, and 3 real elements plus 3*2556 complex elements for HV polarisation. These quantities shall be reduced to the same amounts as the previous values by discarding the cross-polar measurements of LICEF-NIR elements in dual polarisation, and by data combination as described in [RD.2] in the case of full pol scenes.

3.4. AUX_RFI_LST

This module is the only module in L1PP that is not data driven, that is, the user must configure L1PP (through its configuration file) in order to perform the detection algorithm. The only output of this module is a binary file with a statistical distribution of the position and average BTs of the RFIs observed in the data fed to L1PP. The detection algorithms are performed inside the Foreign Sources module, after applying the Sun Direct correction.

A high level description of the algorithm is represented by Figure 13.

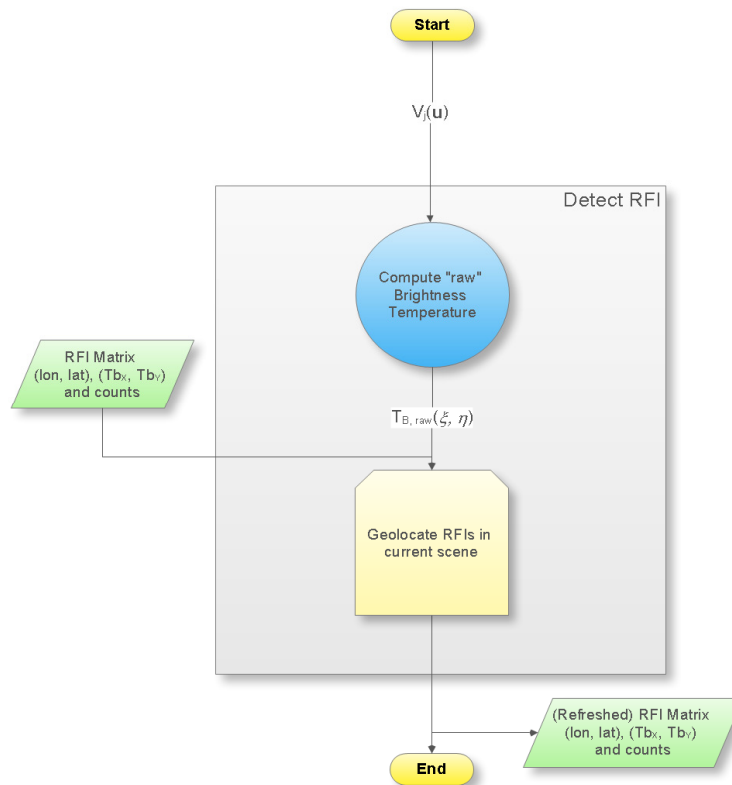


Figure 13: High level description of Detect RFI Algorithm

For each SMOS L1a product, this algorithm updates³ a matrix indexed by the geographical coordinates, number of hits and BT of RFIs for all observations comprehended in a given range of temperatures.

The geolocation of RFIs is done for each scene in the product and a high level description of the algorithm is shown in Figure 14.

The RFI BT is computed as a running average of the $max(T_{B, Raw})$ and it is annotated as $T_{B,X}$ and $T_{B,Y}$ in the output histogram.

³ Or creates it, if the algorithm is being run for the first time.

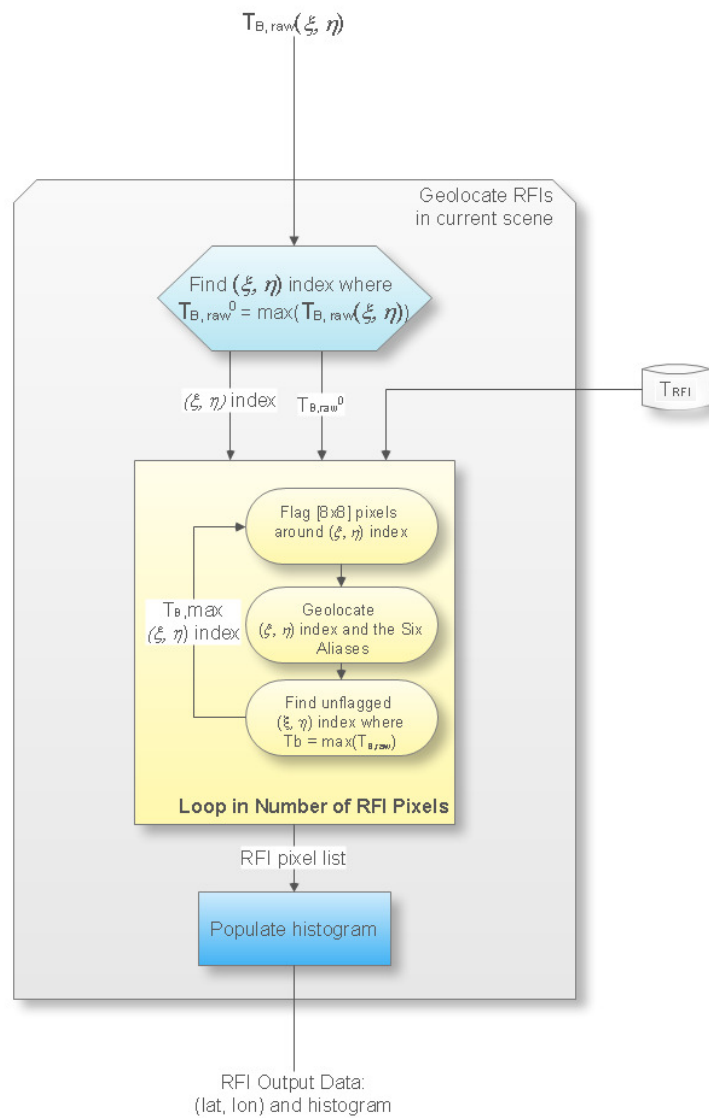


Figure 14: Identification of RFIs and Geolocalisation in the Detection Algorithms

The binary file generated will be used to populate the new ADF that contains a List of RFI sources.

3.5. RFI Detection Algorithms

The detection algorithms are packed in two functions: detectRfiPosition and logRfiPosition, which are described in this section.

3.5.1. detectRFIPosition Function

3.5.1.1. Inputs

- Calibrated Visibilities
- RFI Matrix

3.5.1.2. Outputs

- RFI Histogram

3.5.1.3. List of Variables

The following table describes the variables used in the subsequent implementation section. Variables are listed as input, local and output (I, L, O). The *Size* column indicates the number of elements constituting that variable, and NOT the size of the variable in bytes (this information can be taken from the *Type* column).

| Variable name | Description | Definition | Type | Class | Unit | Size |
|---------------------------------|--|---------------|--------------------|-------|------|---------------------|
| processing_flags | Structure containing processing flags | Sec. 4.3.3. | t_processing_flags | I | N/A | 1 |
| l1b_visibs_data | Calibrated visibilities in L1b format | Sec. 3.1 | double | I | K | 9390(D) 15996(F) |
| time_id | EE CFI time structure | | xl_time_id | I | | 1 |
| attitude_id | EE CFI pointing structure | | xp_attitude_id | I | | 1 |
| l1b_ftt_data | Flat Target data in L1b format | Sec. 2.2.2.2. | double | I | K | 9390(D) 15996(F) |
| weight_visibs | Weights to be applied to each baseline | N/A | double | I | N/A | 9390(D) 15996(F) |
| lice_f_coordinates_data_pointer | LICEF Coordinates | N/A | double | I | N/A | Pointer |
| rfi_output_data | Structure with information on the RFI pixels | | t_l1b_rfi_data | I+O | N/A | [Nbr RFIs in Scene] |

Table 7: detectRFIPosition variable list (Local variables list tbc)

3.5.1.4. Implementation

The function *detectRFIPosition* is run inside the Foreign Sources module, for each scene in the product the detection algorithm is performed.

It starts by computing a distribution of brightness temperature in the snapshot according to Eq. 12,

$$T_{Raw}^{pq}(\xi, \eta) = F^{-1}(V^{pq}(u, v) - V_{Rec}^{pq}(u, v)) \quad \text{Eq. 12}$$

where

$T_{Raw}^{pq}(\xi, \eta)$ - is the “raw” brightness temperature image;

$V^{pq}(u, v)$ - corresponds to the calibrated L1a visibilities;

$V_{Rec}^{pq}(u, v)$ - is the receivers visibilities, computed as $V_{Rec}^{pq}(u, v) = \frac{T_{Rec} V_{FTT}^{pq}(u, v)}{|T_{Ref,FTT} - T_{Rec,FTT}|}$;

The detection of RFI is done for every (ξ, η) pixel in the scene, being the limits imposed by:

- A minimum value, T_{RFI} , which will be configurable by the user in the L1PP configuration file; and
- A maximum value, defined as a fraction of T_{Raw}^{pq} .
- A zone defined by the user in the configuration file (either the whole Unit-Circle or strickly the Alias Free Field of View).

Due to the definition of the (ξ, η) grid and because most of the RFIs are not point-like sources, the surrounding pixels of a RFI-detected-pixel are discarded within a square of NxN, where N is determined according to the strength of the RFI-detected-pixel. This means that for every RFI source detected, L1PP will not detect any other RFI in that snapshot on the NxN pixels around the source, in order to avoid detection of sidelobes from strong sources.

3.5.2. logRFIPosition Function

After processing all the scenes in a single product, the RFI positions are determined based on the output data from the previous function.

3.5.2.1. Inputs

- RFI Histogram

3.5.2.2. Outputs

- RFI Matrix – Binary file written with the number of events for RFI positions

3.5.2.3. List of Variables

The following table describes the variables used in the subsequent implementation section. Variables are listed as input, local and output (I, L, O). The *Size* column indicates the number of elements constituting that variable, and NOT the size of the variable in bytes (this information can be taken from the *Type* column).

| Variable name | Description | Definition | Type | Class | Unit | Size |
|-------------------|---|------------|----------------|-------|------|---------------------|
| rfi_output_data | Structure with information on the RFI pixels | N/A | t_11b_rfi_data | I | N/A | [Nbr RFIs in Scene] |
| RFI_Histogram.dbl | Binary file with the RFI <i>all</i> positions | N/A | double | O | N/A | 3*[LINES xCOLS] |
| RFI Positions | Most probable RFI positions in geographic coordinates | N/A | log | O | N/A | |

Table 8: logRFIPosition variable list (Local variables list tbc)

3.5.2.4. Implementation

The function *logRFIPosition* is run after the Foreign Sources and Error Mitigation modules. It consists in filtering the results in the structure **rfi_output_data** and writing a binary file that contains all the RFI detected in the processed product.

The RFI accurate position is written in the logs and determined based on the distribution of the number of hits around each (i, j) pair of indices for the **rfi_output_data** structure. To avoid identifying the same RFI twice, a lower threshold of N_{counts} is established. The upper limit in this threshold is defined as 1/6 of the maximum number of hits found in the RFI_Histogram.dbl product.

The size of the RFI_Histogram.dbl is hardcoded in L1PP as [1440x720], which corresponds to a cellsize of [0.25x0.25] degrees.

4. L1PP ADF CONTENTS

The following table summarises the origin of the data contained in each ADF, specific tools used in its generation and special procedures followed (if any):

Table 9: Generation Procedures Auxiliary Data Files

| Type of Data | Origin of Data | Specific Tools | Procedure |
|--|---|----------------|--|
| AUX_APDL_ AUX_APDS_ | Blackmann function equation Eq. 17 of DPM LIC | None | Generated manually by DEIMOS. Fixed file so it had to be generated only once. |
| Best Fit Plane (AUX_BFP) | On-ground measurement data provided by EADS CASA Espacio with MIRAS Database v2.2 In-orbit measurements provided by CESBIO (F. Cabot) | None | Generated manually by DEIMOS. |
| Bistatic Scattering Coefficients (AUX_BSCAT) | Look-Up-Table provided by IFREMER. | None | Generated manually by DEIMOS. Fixed file so it had to be generated only once. |

| Type of Data | Origin of Data | Specific Tools | Procedure |
|-------------------------------------|---|---|---|
| IERS Bulletin B File | File provided by SMOS FOS | None | None |
| Baseline Weights (AUX_BWGHT) | Suppressed baselines defined during KP3 (weight set to zero) NIR-LICEF baselines provided by OBS-MIP (E. Anterrieu) | None | Generated manually by DEIMOS. |
| Discrete Global Grid (AUX_DGG) | ISEA aperture 4, resolution 9 global hexagonal grid (4H9), generated by DGGRID GETASSE30 used for the altitude computation of each grid cell | DGGRID Software (http://webpages.sou.edu/~sahrk/dgg/dggrid/dggrid.html) Modified DGGRID instance for binning GETASSE30 DEM into ISEA | Generated by DEIMOS using the available tools |
| Failing Components Table (AUX_FAIL) | No elements set to fail | None | Generated manually by DEIMOS. |

| Type of Data | Origin of Data | Specific Tools | Procedure |
|--|---|------------------------------------|--|
| Galaxy L-band Map (AUX_GALAXY) | <p>Values of the first 4 layers have been taken directly from the map produced by ESA (N. Floury, 15-01-2008 v2.1)</p> <p>Final two layers representing the NIR expected measurements and RMS values that are used in NIR calibration and FTT were provided by EADS CASA Espacio.</p> | Matlab script developed by DEIMOS. | Generated manually by DEIMOS using available tool. |
| Receivers Characterisation (AUX_LCF) | <p>On-ground measurement data provided by EADS CASA Espacio with MIRAS Database v2.2 and updated with latest LICEF antenna model coefficients.</p> | None | Generated manually by DEIMOS. |

| Type of Data | Origin of Data | Specific Tools | Procedure |
|--|---|---|---|
| Land/Sea Mask (AUX_LSMASK) | <p>USGS LandSea Mask (http://edc2.usgs.gov/1KM/and_sea_mask.php) binned to ISEA 4H9 grid</p> <p>MERIS Hierarchical Coastline data provided by Brockman Consulting</p> | <p>Modified DGGRID instance for binning USGS LandSea Mask into ISEA</p> <p>Ad-hoc C99 tool created to combine USGS binning and MERIS coastline data into final binary file.</p> | Generated by DEIMOS using the available tools (first USGS binning, then adding the hierarchical coastlines) |
| L1C Pixel Mask (AUX_MASK) | List of pixels to be stored in SM or OS products was provided by L2 teams | Ad-hoc C99 tool created to combine OS and SM pixel lists into final binary file. | Generated by DEIMOS using the available tool |
| Mispointing Angles (AUX_MISP) | On-ground measurement data provided by EADS CASA Espacio with MIRAS Database v2.2 | None | Generated manually by DEIMOS. |
| Moon Brightness Temperature Map Model (AUX_MOONT) | Data currently not available | None | Generated manually by DEIMOS with placeholder values. |

| Type of Data | Origin of Data | Specific Tools | Procedure |
|--|--|----------------|-------------------------------|
| NIR Characterisation tables (AUX_NIR) | On-ground measurement data provided by EADS CASA Espacio with MIRAS Database v2.2 Data refined with latest NIR antenna model evolution from HUT (J. Kainulainen) | None | Generated manually by DEIMOS. |
| PLM Characterisation Table (AUX_PLM) | On-ground measurement data provided by EADS CASA Espacio with MIRAS Database v2.2 | None | Generated manually by DEIMOS. |
| PMS Characterisation tables (AUX_PMS) | On-ground measurement data provided by EADS CASA Espacio with MIRAS Database v2.2 Date refined with latest PMS heater delay calibration campaign from UPC. | None | Generated manually by DEIMOS. |

| Type of Data | Origin of Data | Specific Tools | Procedure |
|---|---|----------------|---|
| RFI sources Map (AUX_RFI) | Data currently not available (dummy file) | None | Generated manually by DEIMOS with placeholder values. |
| RFI Sources List (AUX_RFILIST) | File provided by L2 contractor (ARRAY) | None | None. |
| Relevant S-parameters of MIRAS (AUX_SPAR) | On-ground measurement data provided by EADS CASA Espacio with MIRAS Database v2.2 | None | Generated manually by DEIMOS. |
| Sun Brightness Temperature Map Model (AUX_SUNT) | Data currently not available | None | Generated manually by DEIMOS with placeholder values. |
| Reference Orbit Scenario File | File provided by SMOS FOS | None | None |
| Average Antenna Patterns (AUX_PATT)) | On-ground measurement data provided by EADS CASA Espacio with MIRAS Database v2.2 | None | Generated manually by DEIMOS. |

5. AUXILIARY DATA FILES

The following tables identify the ADFs ingested by L1PP v6.0.0 and provide relevant information about these files. An specific statement is included about the applicability of each file to the Launch Baseline or not, depending on whether the file is ready to be used, or if there is no Launch Baseline yet.

As of post-Launch version v3.3.0 of L1PP, no FTTx are provided in the ADF TDS, as the formal baseline is available from other sources within DPGS (as is the case for other operational products like GMAT, JMAT and ANIR, which are not considered ADF and thus not provided in this TDS). In addition, IVT and SEPS ADF distribution has been discontinued, only Post-Launch ADF shall be provided during the operations phase.

Despite the fact that all the files have “.EEF” extension, some of them are pure XML files instead of “Hybrid” composed of an XML Header and a Binary Data Block. Tables 4 and 5 contain a column describing the internal format of the file, which can be:

EEF – Hybrid Files containing an XML Header and a Binary Data Block;

XML - Pure XML Files, following the Earth Explorer File Format Standard.

Table 10: List of Auxiliary Data Files

| Type of Data | Description | File Name | Size | Format |
|---------------------------------|--|---|---------|--------|
| Apodisation Window Coefficients | Defines the apodisation function coefficients over the frequency domain coordinates (U,V) for the Blackman Window. Launch Baseline | SM_TEST_AUX_APDL____20070101T000000_20500101T000000_300_001_0.EEF | 216 027 | XML |
| | | SM_TEST_AUX_APDS____20070101T000000_20500101T000000_300_001_0.EEF | 216 026 | |

| Type of Data | Description | File Name | Size | Format |
|----------------------------------|---|--|------------------|--------|
| Best Fit Plane | Euler Rotation Angles between Antenna Reference Frame and Best-Fit Plane. Filled with on-ground calibrated BFP and first in-orbit calibrated BFP. Post-Launch (KP2) Baseline | SM_TEST_AUX_BFP____20050101T000000_20500101T000000_340_001_0.EEF | 2 508 | XML |
| Bistatic Scattering Coefficients | Bistatic Scattering Coefficients used for removing Sun Glint effects. Look-Up-Table provided by IFREMER. Launch Baseline | SM_TEST_AUX_BSCAT__20070101T000000_20500101T000000_300_001_0 | 832 352 | EEF |
| IERS Bulletin B File | Bulletin B Earth Orientation parameters, linking UTC time to UT1, TAI and GPS time. Generated by IERS File provided for completeness and reproduction of LIPP TDS results. LIPP is not the official provider of this file. Post-Launch Baseline | SM_TEST_AUX_BULL_B_20100202T000000_20100301T235959_100_001_3 SM_TEST_AUX_BULL_B_20101202T000000_20110101T235959_100_001_3 | 16 553 17 546 | EEF |

| Type of Data | Description | File Name | Size | Format |
|---------------------------------|--|--|------------|--------|
| Baseline Weights | Baseline weights used during Image Reconstruction to alter the relative weight of certain baselines First in-orbit characterisation of NIR-LICEF weights, plus hinge baselines and NIR-NIR baselines across arms are suppressed (weight set to 0) Post-Launch (KP3) Baseline. The baseline formed by NIR AB has also been removed. | SM_TEST_AUX_BWGT__20070101T000000_20500101T000000_340_004_0.EEF | 337 023 | XML |
| L1 Algorithm Configuration File | Unified L1 algorithm configuration file, containing L1 science and calibration configurations. Post-Launch Baseline. | SM_TEST_AUX_CNFL1P_20110501T000000_20500101T000000_600_001_3.EEF | 14 755 | XML |
| Discrete Global Grid | ISEA aperture 4, resolution 9 global hexagonal grid, containing geodetic coordinates (lat-lon-alt) of all pixels. Launch Baseline | SM_TEST_AUX_DGG____20070101T000000_20500101T000000_300_001_0 | 41 943 320 | EEF |
| Failing Components Table | Failing components table set to no failures in any element, except for NIR-AB, as per QWG-3 recommendation. Post-Launch Baseline | SM_TEST_AUX_FAIL__20070101T000000_20500101T000000_300_002_0.EEF | 51 275 | XML |

| Type of Data | Description | File Name | Size | Format |
|----------------------------|---|---|------------------------------------|--------|
| Galaxy L-band Map | <p>Map of the Galaxy Brightness Temperatures containing 6 layers of 721x1441 elements. Values of the first 4 layers have been taken directly from the map produced by ESA (N. Floury), plus two additional layers representing the NIR expected measurements and RMS values that are used in NIR calibration and FTT. All values contain the latest baseline available from ESA, including cross-polar measurements above -20° declination. Launch Baseline</p> | SM_TEST_AUX_GLXY____20070101T000000_20781231T235959_000000008.EEF | 24 938 293 | EEF |
| | | <p>SM_TEST_AUX_GALAXY_20070101T000000_20500101T000000_300_002_0</p> <p>SM_TEST_AUX_GALNIR_20070101T000000_20500101T000000_300_001_0</p> | <p>16 623 376</p> <p>8 311 688</p> | |
| Receivers Characterisation | <p>Receivers characterisation (ohmic efficiency and absolute phase). First version of in-orbit characterised antenna efficiency values after changing the LICEF antenna model. Post-Launch Baseline</p> | SM_TEST_AUX_LCF____20050101T000000_20500101T000000_360_003_0 | 88 626 | XML |

| Type of Data | Description | File Name | Size | Format |
|---------------------------------------|---|--|------------|--------|
| Land/Sea Mask | ADF extracted from combining the USGS Land-Sea mask and ISEA grid. Launch Baseline | SM_TEST_AUX_LSMASK_20070101T000000_20500101T000000_300_002_0 | 15 728 820 | EEF |
| LIC Pixel Mask | ADF extracted from combination of Land-Sea Mask flags. This mask contains the latest baseline agreed with L2 teams, including the 200km overlap over coastlines. Launch Baseline | SM_TEST_AUX_MASK_20070101T000000_20500101T000000_300_001_0 | 13 107 370 | EEF |
| Mispointing Angles | ADF containing measured or estimated mispointing angles between the Star Tracker unit and the PLM Launch Baseline | SM_TEST_AUX_MISP_20070101T000000_20500101T000000_300_002_0.EEF | 2 744 | XML |
| Moon Brightness Temperature Map Model | Moon Brightness Temperature measurements, to be used only for reprocessing. ADF currently incomplete. Launch Baseline | SM_TEST_AUX_MOONT_20070101T000000_20500101T000000_300_001_0 | 2 617 | EEF |

| Type of Data | Description | File Name | Size | Format |
|-----------------------------------|--|--|--------|--------|
| NIR Characterisation tables | NIR characterisation table. All values measured on- ground have been incorporated into this baseline Fourth version of in-orbit characterised sensitivity values, including new NIR drift parameters. Post-Launch Baseline | SM_TEST_AUX_NIR____20070101T000000_20500101T000000_350_004_0.EEF | 15 135 | XML |
| PLM Characterisation Table | Parameters calibrated on- ground referent to elements of the PLM. Version 300_005 and onwards must be used with in-orbit data due to the differences in central frequency. Version 600 contains new antenna pattern renormalisation factors. Post-Launch Baseline | SM_TEST_AUX_PLM____20070101T000000_20500101T000000_600_001_0.EEF | 54 097 | XML |

| Type of Data | Description | File Name | Size | Format |
|-----------------------------|--|--|------------|--------|
| PMS Characterisation tables | PMS characterisation table, computed on-ground. Second Order Sensitivities have been set to zero according to KP2 recommendation. Third in-orbit characterisation of PMS Heater delays. First in-orbit characterisation of PMS Sensitivities. Version 600 contains new Receiver Noise Temperature fields from original MIER measurements. Post-Launch Baseline | SM_TEST_AUX_PMS____20050101T000000_20500101T000000_600_001_0.EEF | 129 570 | XML |
| RFI sources Map | ADF containing TRUE values for those pixels that are expected to be affected by RFI. Issue 2 is filled completely with zeros. Launch Baseline | SM_TEST_AUX_RFI____20070101T000000_20500101T000000_300_002_0 | 13 107 370 | EEF |

| Type of Data | Description | File Name | Size | Format |
|--------------------------------|---|--|--|------------|
| RFI Sources List | <p>ADF containing the list of global RFI sources (position, expected strength and applicable flags during L1 processing)</p> <p>Third operational file provided by L2 contractor, contains all RFI sources to be flagged and none to be mitigated.</p> <p>Post-Launch Baseline</p> | <p>SM_TEST_AUX_RFILST_20070101T000000_20500101T000000_360_003_0.EEF</p> | <p>111 768</p> | <p>XML</p> |
| Relevant S-parameters of MIRAS | <p>Noise distribution networks and switch S-parameters characterisation.</p> <p>NDN data has been filled with complete data from EADS CASA Espacio with the full S-parameters and corrections from UPC.</p> <p>Switch data has been filled using EADS CASA Espacio measurements.</p> <p>Third in-orbit characterisation of CAS correction factors, applicable to different dates.</p> <p>Post-Launch Baseline</p> | <p>SM_TEST_AUX_SPAR___20050101T000000_20100111T120700_340_005_0.EEF</p> <p>SM_TEST_AUX_SPAR___20100111T120700_20110112T091500_340_006_0.EEF</p> <p>SM_TEST_AUX_SPAR___20110112T091500_20500101T000000_340_007_0.EEF</p> | <p>1 456 315</p> <p>1 456 315</p> <p>1 456 315</p> | <p>XML</p> |

| Type of Data | Description | File Name | Size | Format |
|--------------------------------------|---|--|-------------|--------|
| Sun Brightness Temperature Map Model | Sun Brightness Temperature measurements, to be used only for reprocessing. ADF currently incomplete. Launch Baseline | SM_TEST_AUX_SUNT___20070101T000000_20500101T000000_300_001_0 | 2 616 | EEF |
| Reference Orbit Scenario File | Reference orbit description, linking UTC time to orbit time. Generated using EE CFI Function. File provided for completeness and reproduction of L1PP TDS results. L1PP is not the official provider of this file. Post-Launch Baseline | SM_TEST_MPL_ORBSCT_20091102T031142_20500101T000000_350_003_1.EEF | 13 369 | XML |
| Average Antenna Patterns | Post-Launch baseline for Antenna Patterns, including corrected xi-eta coordinates annotation and latest averaging and normalization algorithm using only 69 antennas (not duplicating NIR-LICEF patterns). Post-Launch Baseline | SM_TEST_AUX_PATT___20070101T000000_20500101T000000_320_003_0 | 457 613 144 | EEF |

6. ANNEX: ADF SET PACKAGE CONTENTS

```
├──adf-dpgs  
└──adf-eef
```

```
data/  
adf-dpgs  
adf-eef
```

```
data/adf-dpgs:  
SM_TEST_AUX_APDL____20070101T000000_20500101T000000_300_002_0.EEF  
SM_TEST_AUX_APDS____20070101T000000_20500101T000000_300_002_0.EEF  
SM_TEST_AUX_BFP____20070101T000000_20500101T000000_340_001_0.EEF  
SM_TEST_AUX_BSCAT____20070101T000000_20500101T000000_300_001_0  
SM_TEST_AUX_BULL_B_20100202T000000_20100301T235959_100_001_3  
SM_TEST_AUX_BULL_B_20101202T000000_20110101T235959_100_001_3  
SM_TEST_AUX_BWGHT____20050101T000000_20500101T000000_340_004_4.EEF  
SM_TEST_AUX_CNFL1P_20110501T000000_20500101T000000_600_001_0.EEF  
SM_TEST_AUX_DGG____20070101T000000_20500101T000000_300_001_0  
SM_TEST_AUX_FAIL____20070101T000000_20500101T000000_300_002_0.EEF  
SM_TEST_AUX_GALAXY_20070101T000000_20500101T000000_300_002_0  
SM_TEST_AUX_GALNIR_20070101T000000_20500101T000000_300_001_0  
SM_TEST_AUX_LCF____20050101T000000_20500101T000000_360_003_0.EEF  
SM_TEST_AUX_LSMASK_20070101T000000_20500101T000000_300_002_0  
SM_TEST_AUX_MASK____20070101T000000_20500101T000000_300_001_0  
SM_TEST_AUX_MISP____20070101T000000_20500101T000000_300_002_0.EEF  
SM_TEST_AUX_MOONT____20070101T000000_20500101T000000_300_001_0  
SM_TEST_AUX_NIR____20070101T000000_20500101T000000_350_004_0.EEF  
SM_TEST_AUX_PATT____20070101T000000_20500101T000000_320_003_0  
SM_TEST_AUX_PLM____20070101T000000_20500101T000000_600_001_0.EEF  
SM_TEST_AUX_PMS____20050101T000000_20500101T000000_600_001_0.EEF  
SM_TEST_AUX_RFI____20070101T000000_20500101T000000_300_002_0  
SM_TEST_AUX_RFILST_20070101T000000_20500101T000000_360_003_0.EEF  
SM_TEST_AUX_SPAR____20050101T000000_20100111T120700_340_005_0.EEF  
SM_TEST_AUX_SPAR____20100111T120700_20110112T091500_340_006_0.EEF  
SM_TEST_AUX_SPAR____20110112T091500_20500101T000000_340_007_0.EEF  
SM_TEST_AUX_SUNT____20070101T000000_20500101T000000_300_001_0  
SM_TEST_MPL_ORBSC_20091102T031142_20500101T000000_350_003_1.EEF
```

```
data/adf-dpgs/SM_TEST_AUX_BULL_B_20100202T000000_20100301T235959_100_001_3:  
SM_TEST_AUX_BULL_B_20100202T000000_20100301T235959_100_001_3.DBL  
SM_TEST_AUX_BULL_B_20100202T000000_20100301T235959_100_001_3.HDR
```

```
data/adf-dpgs/SM_TEST_AUX_BULL_B_20101202T000000_20110101T235959_100_001_3:  
SM_TEST_AUX_BULL_B_20101202T000000_20110101T235959_100_001_3.DBL  
SM_TEST_AUX_BULL_B_20101202T000000_20110101T235959_100_001_3.HDR
```

```
data/adf-dpgs/SM_TEST_AUX_DGG____20070101T000000_20500101T000000_300_001_0:  
SM_TEST_AUX_DGG____20070101T000000_20500101T000000_300_001_0.DBL  
SM_TEST_AUX_DGG____20070101T000000_20500101T000000_300_001_0.HDR
```

```
data/adf-dpgs/SM_TEST_AUX_GALAXY_20070101T000000_20500101T000000_300_002_0:  
SM_TEST_AUX_GALAXY_20070101T000000_20500101T000000_300_002_0.DBL  
SM_TEST_AUX_GALAXY_20070101T000000_20500101T000000_300_002_0.HDR
```

```
data/adf-dpgs/SM_TEST_AUX_GALNIR_20070101T000000_20500101T000000_300_001_0:  
SM_TEST_AUX_GALNIR_20070101T000000_20500101T000000_300_001_0.DBL  
SM_TEST_AUX_GALNIR_20070101T000000_20500101T000000_300_001_0.HDR
```

```
data/adf-dpgs/SM_TEST_AUX_LSMASK_20070101T000000_20500101T000000_300_002_0:  
SM_TEST_AUX_LSMASK_20070101T000000_20500101T000000_300_002_0.DBL
```

SM_TEST_AUX_LSMASK_20070101T000000_20500101T000000_300_002_0.HDR

data/adf-dpgs/SM_TEST_AUX_MASK____20070101T000000_20500101T000000_300_001_0:
SM_TEST_AUX_MASK____20070101T000000_20500101T000000_300_001_0.DBL
SM_TEST_AUX_MASK____20070101T000000_20500101T000000_300_001_0.HDR

data/adf-dpgs/SM_TEST_AUX_MOONT____20070101T000000_20500101T000000_300_001_0:
SM_TEST_AUX_MOONT____20070101T000000_20500101T000000_300_001_0.DBL
SM_TEST_AUX_MOONT____20070101T000000_20500101T000000_300_001_0.HDR

data/adf-dpgs/ SM_TEST_AUX_PATT____20050101T000000_20500101T000000_320_003_0:
SM_TEST_AUX_PATT____20050101T000000_20500101T000000_320_003_0.DBL
SM_TEST_AUX_PATT____20050101T000000_20500101T000000_320_003_0.HDR

data/adf-dpgs/SM_TEST_AUX_RFI____20070101T000000_20500101T000000_300_002_0:
SM_TEST_AUX_RFI____20070101T000000_20500101T000000_300_002_0.DBL
SM_TEST_AUX_RFI____20070101T000000_20500101T000000_300_002_0.HDR

data/adf-dpgs/SM_TEST_AUX_SUNT____20070101T000000_20500101T000000_300_001_0:
SM_TEST_AUX_SUNT____20070101T000000_20500101T000000_300_001_0.DBL
SM_TEST_AUX_SUNT____20070101T000000_20500101T000000_300_001_0.HDR

data/adf-eef:
SM_TEST_AUX_GLXY____20070101T000000_20781231T235959_00000008.EEF